

UC San Diego

UC San Diego Previously Published Works

Title

Physical Model Tests of Half-Scale Geosynthetic Reinforced Soil Bridge Abutments. I: Static Loading

Permalink

<https://escholarship.org/uc/item/9q87p31t>

Journal

Journal of Geotechnical and Geoenvironmental Engineering, 145(11)

ISSN

1090-0241

Authors

Zheng, Yewei
Fox, Patrick J
Shing, P Benson
et al.

Publication Date

2019-11-01

DOI

10.1061/(asce)gt.1943-5606.0002152

Peer reviewed

Journal of Geotechnical and Geoenvironmental Engineering

Physical Model Tests of Half-Scale Geosynthetic Reinforced Soil Bridge Abutments. I: Static Loading

--Manuscript Draft--

Manuscript Number:	GTENG-7258R2	
Full Title:	Physical Model Tests of Half-Scale Geosynthetic Reinforced Soil Bridge Abutments. I: Static Loading	
Manuscript Region of Origin:	UNITED STATES	
Article Type:	Technical Paper	
Funding Information:	California Department of Transportation	John McCartney
	Federal Highway Administration	John McCartney
Abstract:	<p>This paper presents experimental results from physical model tests on four half-scale geosynthetic reinforced soil (GRS) bridge abutment specimens constructed using well-graded angular backfill sand, modular facing blocks, and uniaxial geogrid reinforcement to investigate the effects of applied surcharge stress, reinforcement vertical spacing, and reinforcement tensile stiffness for working stress, static loading conditions. Facing displacements increased for the upper section of the walls after the application of surcharge stress and were greater for larger reinforcement vertical spacing and reduced reinforcement tensile stiffness. Bridge seat settlements were proportional to the applied surcharge stress, strongly affected by larger reinforcement vertical spacing, and only slightly affected by reduced reinforcement tensile stiffness. Measured vertical and lateral soil stresses generally were lower than calculated values for static loading conditions. The maximum tensile strain in each reinforcement layer occurred near the facing block connection for lower layers and under the bridge seat for higher layers. A companion paper presents experimental results for the same GRS bridge abutment specimens under dynamic loading conditions.</p>	
Corresponding Author:	Yewei Zheng, PhD Old Dominion University Norfolk, Virginia UNITED STATES	
Corresponding Author E-Mail:	y1zheng@odu.edu;zhengyewei@gmail.com	
Order of Authors:	Yewei Zheng, PhD	
	Patrick Fox, PhD	
	Benson Shing, PhD	
	John McCartney, PhD	
Additional Information:		
Question	Response	
Authors are required to attain permission to re-use content, figures, tables, charts, maps, and photographs for which the authors do not hold copyright. Figures created by the authors but previously published under copyright elsewhere may require permission. For more information see http://ascelibrary.org/doi/abs/10.1061/9780784479018.ch03 . All permissions must be uploaded as a permission file in PDF format. Are there any required permissions that have not yet been	No	

secured? If yes, please explain in the comment box.	
ASCE does not review manuscripts that are being considered elsewhere to include other ASCE Journals and all conference proceedings. Is the article or parts of it being considered for any other publication? If your answer is yes, please explain in the comments box below.	No
Is this article or parts of it already published in print or online in any language? ASCE does not review content already published (see next questions for conference papers and posted theses/dissertations). If your answer is yes, please explain in the comments box below.	No
Has this paper or parts of it been published as a conference proceeding? A conference proceeding may be reviewed for publication only if it has been significantly revised and contains 50% new content. Any content overlap should be reworded and/or properly referenced. If your answer is yes, please explain in the comments box below and be prepared to provide the conference paper.	No
<p>ASCE allows submissions of papers that are based on theses and dissertations so long as the paper has been modified to fit the journal page limits, format, and tailored for the audience. ASCE will consider such papers even if the thesis or dissertation has been posted online provided that the degree-granting institution requires that the thesis or dissertation be posted.</p> <p>Is this paper a derivative of a thesis or dissertation posted or about to be posted on the Internet? If yes, please provide the URL or DOI permalink in the comment box below.</p>	Yes
<p>If yes, please provide the URL or DOI permalink in the comment box below.</p> <p>as follow-up to "ASCE allows submissions of papers that are based on theses and dissertations so long as the paper has been modified to fit the journal</p>	<p>https://escholarship.org/uc/item/0vg5b2g4</p>

<p>page limits, format, and tailored for the audience. ASCE will consider such papers even if the thesis or dissertation has been posted online provided that the degree-granting institution requires that the thesis or dissertation be posted.</p> <p>Is this paper a derivative of a thesis or dissertation posted or about to be posted on the Internet? If yes, please provide the URL or DOI permalink in the comment box below."</p>	
<p>Each submission to ASCE must stand on its own and represent significant new information, which may include disproving the work of others. While it is acceptable to build upon one's own work or replicate other's work, it is not appropriate to fragment the research to maximize the number of manuscripts or to submit papers that represent very small incremental changes. ASCE may use tools such as CrossCheck, Duplicate Submission Checks, and Google Scholar to verify that submissions are novel. Does the manuscript constitute incremental work (i.e. restating raw data, models, or conclusions from a previously published study)?</p>	No
<p>Authors are expected to present their papers within the page limitations described in Publishing in ASCE Journals: A Guide for Authors. Technical papers and Case Studies must not exceed 30 double-spaced manuscript pages, including all figures and tables. Technical notes must not exceed 7 double-spaced manuscript pages. Papers that exceed the limits must be justified. Grossly over-length papers may be returned without review. Does this paper exceed the ASCE length limitations? If yes, please provide justification in the comments box below.</p>	No
<p>All authors listed on the manuscript must have contributed to the study and must approve the current version of the manuscript. Are there any authors on the paper that do not meet these criteria? If the answer is yes, please explain in the comments.</p>	No

Was this paper previously declined or withdrawn from this or another ASCE journal? If so, please provide the previous manuscript number and explain what you have changed in this current version in the comments box below. You may upload a separate response to reviewers if your comments are extensive.	No
Companion manuscripts are discouraged as all papers published must be able to stand on their own. Justification must be provided to the editor if an author feels as though the work must be presented in two parts and published simultaneously. There is no guarantee that companions will be reviewed by the same reviewers, which complicates the review process, increases the risk for rejection and potentially lengthens the review time. If this is a companion paper, please indicate the part number and provide the title, authors and manuscript number (if available) for the companion papers along with your detailed justification for the editor in the comments box below. If there is no justification provided, or if there is insufficient justification, the papers will be returned without review.	<p>Ref.:Submittal of companion papers: "Physical Model Tests on Half-Scale Geosynthetic Reinforced Soil Bridge Abutments. I: Static Loading." by Y. Zheng, P.J. Fox, P.B. Shing, and J.S. McCartney and "Physical Model Tests on Half-Scale Geosynthetic Reinforced Soil Bridge Abutments. II: Dynamic Loading." by Y. Zheng, P.J. Fox, P.B. Shing, and J.S. McCartney for possible publication as Technical Papers in ASCE Journal of Geotechnical and Geoenvironmental Engineering</p> <p>Dear Editor,</p> <p>Please find enclosed our companion manuscripts submitted for review and possible publication as technical papers in Journal of Geotechnical and Geoenvironmental Engineering. The papers focus on physical model tests on geosynthetic reinforced soil (GRS) bridge abutments. We believe that the papers work well as a companion set because the first paper presents the experimental program and static response of GRS bridge abutments, while the second paper presents the dynamic response for a series of earthquake motions in the longitudinal direction.</p> <p>Please contact me should you need any clarification. I look forward to having this paper published in Journal of Geotechnical and Geoenvironmental Engineering.</p> <p>Best regards, Yewei Zheng</p>
If this manuscript is intended as part of a Special Issue or Collection, please provide the Special Collection title and name of the guest editor in the comments box below.	
Recognizing that science and engineering are best served when data are made available during the review and discussion of manuscripts and journal articles, and to allow others to replicate and build on work published in ASCE journals, all reasonable requests by reviewers for materials, data, and associated protocols must be fulfilled. If you are restricted from sharing your data and materials, please explain below.	
Papers published in ASCE Journals must make a contribution to the core body of knowledge and to the advancement of the field. Authors must consider how their	This paper presents experimental data on the static response of half-scale GRS bridge abutments during construction stages, including wall facing displacements, bridge seat settlements, vertical and lateral soil stresses, and reinforcement tensile strains.

<p>new knowledge and/or innovations add value to the state of the art and/or state of the practice. Please outline the specific contributions of this research in the comments box.</p>	
<p>The flat fee for including color figures in print is \$800, regardless of the number of color figures. There is no fee for online only color figures. If you decide to not print figures in color, please ensure that the color figures will also make sense when printed in black-and-white, and remove any reference to color in the text. Only one file is accepted for each figure. Do you intend to pay to include color figures in print? If yes, please indicate which figures in the comments box.</p>	<p>No</p>
<p>If there is anything else you wish to communicate to the editor of the journal, please do so in this box.</p>	

Physical Model Tests of Half-Scale Geosynthetic Reinforced Soil Bridge Abutments. I: Static Loading

Yewei Zheng, A.M.ASCE¹; Patrick J. Fox, F.ASCE²; P. Benson Shing³, M.ASCE; and John S. McCartney, F.ASCE⁴

Abstract: This paper presents experimental results from physical model tests on four half-scale geosynthetic reinforced soil (GRS) bridge abutment specimens constructed using well-graded angular backfill sand, modular facing blocks, and uniaxial geogrid reinforcement to investigate the effects of applied surcharge stress, reinforcement vertical spacing, and reinforcement tensile stiffness for working stress, static loading conditions. Facing displacements increased for the upper section of the walls after the application of surcharge stress and were greater for larger reinforcement vertical spacing and reduced reinforcement tensile stiffness. Bridge seat settlements were proportional to the applied surcharge stress, strongly affected by larger reinforcement vertical spacing, and only slightly affected by reduced reinforcement tensile stiffness. Measured vertical and lateral soil stresses generally were lower than calculated values for static loading conditions. The maximum tensile strain in each reinforcement layer occurred near the facing block connection for lower layers and under the bridge seat for higher layers. A companion paper presents experimental results for the same GRS bridge abutment specimens under dynamic loading conditions.

Keywords: Geosynthetic reinforced soil; Bridge abutment; Retaining wall; Model test; Static loading.

¹ Assistant Professor, Department of Civil and Environmental Engineering, Old Dominion University, Norfolk, VA 23529 USA (corresponding author). ORCID: <https://orcid.org/0000-0001-9038-4113>. Email: ylzheng@odu.edu

² Shaw Professor and Head, Department of Civil and Environmental Engineering, Pennsylvania State University, University Park, PA 16802 USA. Email: pjfox@engr.psu.edu

³ Professor, Department of Structural Engineering, University of California, San Diego, La Jolla, CA 92093-0085 USA. Email: pshing@ucsd.edu

⁴ Professor and Chair, Department of Structural Engineering, University of California, San Diego, La Jolla, CA 92093-0085 USA. Email: mccartney@ucsd.edu

Introduction

In recent years, geosynthetic reinforced soil (GRS) retaining walls have been adapted to serve as bridge abutments with bridge structure loads applied directly on top of the reinforced soil mass. This technology offers many advantages over traditional pile-supported designs and is becoming widely used for transportation infrastructure applications. Several case histories have been reported for in-service GRS bridge abutments and indicate good performance in terms of facing displacements and bridge seat settlements (Won et al. 1996; Wu et al. 2001; Abu-Hejleh et al. 2002; Adams et al. 2011a; Budge et al. 2014; Saghebfar et al. 2017).

Many experimental studies, including physical model tests and instrumented field structures, have been conducted for GRS walls under static loading conditions (e.g., Runser et al. 2001; Bathurst et al. 2006, 2009; Ehrlich et al. 2012; Ehrlich and Mirmoradi 2013; Allen and Bathurst 2014a, 2014b; Jiang et al. 2016, Mirmoradi and Ehrlich 2017). However, experimental studies on the static behavior of GRS bridge abutments are limited. For example, Abu-Hejleh et al. (2002) measured the field response of the Founders/Meadows GRS bridge abutment in Castle Rock, Colorado, and reported good performance during construction and under service conditions. Similarly, Saghebfar et al. (2017) reported small facing displacements and bridge seat settlements for a GRS-IBS abutment in Louisiana during construction and service. Although these investigations have indicated good field performance of GRS bridge abutments, controlled laboratory tests are needed to evaluate the effects of different design parameters in a systematic manner.

This paper presents experimental results on the static response of four half-scale GRS bridge abutment specimens constructed using well-graded backfill sand, modular facing blocks, and uniaxial geogrid reinforcement to understand the effects of applied surcharge stress,

reinforcement vertical spacing, and reinforcement tensile stiffness for working stress, static loading conditions. Wall facing displacements, bridge seat settlements, soil stresses, and reinforcement tensile strains were measured for different instrumented sections to evaluate multi-directional response. The data illustrate behavior of these structures under service load conditions and can be used for validation of three-dimensional (3D) numerical models. A companion paper (Zheng et al. 2019) presents the dynamic response of the same GRS bridge abutment specimens from shaking table tests for a series of scaled earthquake motions in the longitudinal direction.

Background

Field and laboratory loading tests have been conducted on GRS bridge piers and abutments, and generally indicate relatively small deformations under service load conditions and large bearing capacity (Adams 1997; Gotteland et al. 1997; Ketchart and Wu 1997; Wu et al. 2001, 2006; Lee and Wu 2004; Adams et al. 2011b; Nicks et al. 2013, 2016; Adams et al. 2014; Iwamoto et al. 2015; Xu et al. 2019). Lee and Wu (2004) reviewed the results of several loading tests and suggested that bearing capacity can be as high as 900 kPa for closely spaced geosynthetic reinforcement and well-graded, well-compacted backfill soil. Wu et al. (2006) reported results for full-scale loading tests on a GRS bridge abutment with two instrumented sections in a back-to-back configuration. The two sections were reinforced using woven geotextiles with ultimate strengths of 70 kN/m and 21 kN/m, and the measured abutment compressions were 40 mm and 72 mm, respectively, under an applied vertical stress of 200 kPa. The section with stronger reinforcement did not reach failure for applied vertical stresses in excess of 800 kPa, while the other section with weaker reinforcement experienced excessive deformations for an applied vertical stress of approximately 400 kPa. Nicks et al. (2013, 2016) conducted a series of loading

tests on 2 m-high GRS mini-piers and found that reinforcement vertical spacing and reinforcement strength have the most important effects on the deformation response and ultimate bearing capacity.

Numerical studies also have been conducted for GRS bridge piers and abutments, and generally indicate relatively small facing displacements and bridge seat settlements (e.g., Helwany et al. 2003, 2007; Ambauen et al. 2015; Leshchinsky and Xie 2015; Zheng and Fox 2016, 2017; Ardah et al. 2017; Rong et al. 2017; Abu-Farsakh et al. 2018; Zheng et al. 2018a, 2018b; Shen et al. 2019). Parametric studies indicate that the relative compaction of backfill soil, reinforcement vertical spacing, reinforcement tensile stiffness, and bridge load have the most significant effects on the performance of GRS bridge abutments under static loading (Helwany et al. 2007; Zheng and Fox 2016, 2017). Helwany et al. (2003) found that facing displacements, bridge seat settlements, and differential settlements between the bridge and approach roadway were acceptable for sand and medium-to-stiff clay foundation soils. Zheng and Fox (2016) simulated a full bridge system with GRS bridge abutments on both ends and found that lateral restraining forces due to friction at the bridge structure-bridge seat interface can have an important effect on abutment deformations. Rong et al. (2017) conducted a 3D numerical simulation for a GRS bridge abutment and found that the application of bridge surcharge stress produced multi-directional deformation, including outward displacements of the front wall facing and smaller outward displacements of the side wall facings.

Experimental Program

The experimental program consisted of four GRS bridge abutment specimens, including a baseline case specimen (Specimen 1), a specimen with lower surcharge stress (Specimen 2), a specimen with larger reinforcement vertical spacing (Specimen 3), and a specimen with reduced

reinforcement tensile stiffness (Specimen 4). Details are provided in Table 1, along with the global stiffness of each GRS bridge abutment specimen, as calculated using the method of Bathurst et al. (2009). Values of global stiffness for Specimen 3 and Specimen 4 are approximately equal and one-half of the corresponding value for Specimen 1 and Specimen 2.

Specimen Configuration

The GRS bridge abutment specimens were constructed on the indoor uniaxial servo-hydraulic shaking table in the Charles Lee Powell Structural Research Laboratory at the University of California, San Diego (UCSD), which was refurbished prior to this study to increase the fidelity of dynamic motion (Trautner et al. 2017). Details of the experimental design and specimen construction are provided by Zheng et al. (2018c). The configuration of the GRS bridge abutment system is shown in Figure 1. A concrete beam represents a longitudinal slice of a prototype bridge structure, and rests on a GRS bridge abutment with a concrete bridge seat at one end and on a concrete support wall at the other end. The abutment has modular block facing on three sides, including facing on the front wall (perpendicular to the bridge beam) and the two side walls (parallel to the bridge beam). The back of the abutment specimen was supported by a reaction wall consisting of a steel frame with plywood facing, which was designed to be sufficiently stiff to maintain at-rest lateral earth pressures during construction (Zheng et al. 2018c).

Top and cross-sectional views for the GRS bridge abutment baseline case specimen (Specimen 1) are shown in Figure 2. Horizontal coordinate x is measured toward the south from the back of the front wall facing in the longitudinal section (Figure 2b), horizontal coordinate y is measured toward the east from the back of the west side wall facing in the transverse section (Figure 2c), and vertical coordinate z is measured upward from the top of the foundation soil. The

abutment specimen has plan dimensions of $2.35 \text{ m} \times 2.10 \text{ m}$. The bridge seat has plan dimensions of $0.65 \text{ m} \times 1.30 \text{ m}$ on the bottom surface and a setback distance of 0.15 m from each of the three wall facings. The GRS bridge abutment specimen has a total height of 2.7 m , consisting of a 2.1 m -high lower GRS fill and a 0.6 m -high upper GRS fill, and was constructed on a 0.15 m -thick foundation soil layer placed directly on the shaking table (Zheng et al. 2018c, 2018d). The lower GRS fill consists of fourteen 0.15 m -thick soil lifts, with each lift including reinforcement layers in both the longitudinal and transverse directions. The longitudinal reinforcement layers extend 1.47 m from the front wall facing into the backfill soil. The transverse reinforcement layers extend 0.8 m from each side wall facing to meet, without connection, at the center. The transverse reinforcement layers and side wall facing blocks for each lift are offset by 25 mm vertically from the longitudinal reinforcement layers and front wall facing blocks. Limited by geometry and payload constraints of the shaking table, the retained soil zone (i.e., from the end of longitudinal reinforcement layers to the reaction wall) has a length of 0.63 m and reinforcement layers only in the transverse direction. The upper GRS fill consists of four 0.15 m -thick soil lifts with reinforcement layers only in the transverse direction.

The concrete beam has a weight of 65 kN and dimensions of $6.4 \text{ m} \times 0.9 \text{ m} \times 0.45 \text{ m}$ (length \times width \times height), and the bridge seat has a weight of 7 kN . Additional dead weights (steel plates) equal to 33 kN were evenly distributed and rigidly attached to the concrete beam to produce a total weight of 98 kN . Elastomeric bearing pads with plan dimensions of $0.45 \text{ m} \times 0.90 \text{ m}$ and a thickness of 25 mm were placed under both ends of the beam (Zheng et al. 2018c, 2018d). For Specimens 1, 3, and 4, the total weight of the bridge beam and dead weights produced an average applied surcharge stress of 66 kPa (Table 1) on the lower GRS fill (contact area = 0.85 m^2). For Specimen 2, the concrete beam was used with no additional dead weights and the average applied

surcharge stress on the lower GRS fill was 43 kPa. These surcharge stresses are at the lower end of the typical range, yet representative of service load conditions for GRS bridge abutments supporting a single-span bridge. For example, the GRS-IBS abutment for the Huber Road Bridge reported by Adams et al. (2011a) has a similar applied surcharge stress of 73 kPa.

Soil and Reinforcement

The soil used for construction of the GRS bridge abutment specimens is a clean angular sand, consisting primarily of crushed rock, with no gravel and a low fines content. The sand has coefficient of uniformity $C_u = 6.1$ and coefficient of curvature $C_z = 1.0$ and is classified as well-graded sand (SW) according to the Unified Soil Classification System (USCS). The specific gravity $G_s = 2.61$, the fines content (passing No. 200 sieve) = 2.5%, and the maximum and minimum void ratios are $e_{\max} = 0.853$ and $e_{\min} = 0.371$, respectively (Zheng 2017, Zheng et al. 2018c, 2018d). This sand satisfies the AASHTO and FHWA backfill material requirements for GRS bridge abutments (AASHTO 2012; Adams et al. 2011b). For construction of the GRS bridge abutment specimens, the target backfill soil compaction conditions were gravimetric water content $w_c = 5\%$ and relative density $D_r = 70\%$. This target relative density was selected to meet similitude relationships for 1g shaking table testing, as described in the companion paper (Zheng et al. 2019).

Consolidated-drained triaxial compression tests were performed on dry sand specimens compacted at $D_r = 70\%$ for effective confining stress $\sigma'_3 = 13.8, 34.5, \text{ and } 69.0$ kPa, and the results are shown in Figure 3. The sand has a peak friction angle of $\phi'_p = 51.3^\circ$ and no cohesion. Based on volumetric strains from the point of maximum contraction to an axial strain of 5%, the

average dilation angle $\psi = 13^\circ$ (Zheng et al. 2018c, 2018d). A summary of soil properties is provided in Table 2.

To construct the GRS bridge abutment specimens, the soil was compacted in the unsaturated condition. Unsaturated conditions produce apparent cohesion, which was estimated using the soil-water retention curve (SWRC) and the suction stress concept of Lu et al. (2010). A hanging column test was performed on a sand specimen with $D_r = 70\%$ to measure the drying and wetting path SWRCs, which were fitted using the van Genuchten (1980) model:

$$\theta = \theta_r + (\theta_{\max} - \theta_r) \left[1 + (\alpha_{vG} s)^{N_{vG}} \right]^{-\left(1 - \frac{1}{N_{vG}}\right)} \quad (1)$$

where θ = volumetric water content (volume of water/volume of soil), s = matric suction, θ_{\max} = volumetric water content at zero matric suction for either path, θ_r = residual saturation, and α_{vG} and N_{vG} = model parameters. The measured SWRC data and fitted relationships are shown in Figure 4.

A uniaxial high-density polyethylene (HDPE) geogrid (Tensar LH800) was used as soil reinforcement. Tensile tests were conducted on single rib specimens at a strain rate of 10%/min according to ASTM D6637. Results are shown in Figure 5 and indicate that the geogrid has secant stiffness at 5% strain $J_{5\%} = 380$ kN/m and ultimate strength $T_{ult} = 38$ kN/m in the machine direction, and $J_{5\%} = 80$ kN/m and $T_{ult} = 4$ kN/m in the cross-machine direction. For Specimens 1, 2, and 4, reinforcement was placed with each soil lift to give a vertical spacing $S_v = 0.15$ m. For Specimen 3, reinforcement layers were placed with every other soil lift to give $S_v = 0.3$ m. For Specimen 4, every other rib of the geogrid in the transverse direction was removed to yield a reduced secant stiffness of $J_{5\%} = 190$ kN/m and reduced $T_{ult} = 19$ kN/m.

Construction

A foundation sand layer with a thickness of 0.15 m was first compacted within a perimeter wooden frame on the shaking table and at a higher relative density ($D_r = 85\%$) than the backfill sand to provide a firm base for the GRS bridge abutment. Facings for the front and side walls consisted of concrete modular blocks with plan dimensions of 0.30 m \times 0.25 m and a height of 0.15 m. The first course of the front wall facing blocks was placed and leveled on the foundation layer, with the side wall blocks offset vertically by 25 mm above the front wall blocks. This offset allowed for the placement of a thin (25 mm-thick) soil lift and avoid direct contact between the longitudinal and transverse geogrid layers. This technique was needed to support the front and side walls with uniaxial geogrid, which is generally preferred over biaxial geogrid in seismic regions due to the higher tensile stiffness. As a result of the 25 mm offset, the side wall and front wall facing blocks were not interlocked in a typical masonry pattern at the corners. Geogrid layers were placed between facing blocks with frictional connections and extended horizontally into the backfill soil. Fiberglass pins were used between the blocks for alignment purposes. Although typically grouted in the field (Helwany et al. 2012), the upper course of blocks for each wall remained ungrouted in the current study. The bridge seat was placed on the lower GRS fill and the upper GRS fill was constructed in four lifts using only transverse geogrid layers. Finally, the concrete beam, with or without additional dead weights, depending on the abutment specimen, was placed on the bridge seat and support wall.

Sand cone tests were performed on the compacted backfill soil for selected lifts to measure gravimetric water content and dry unit weight, and random soil samples were collected from each lift to measure gravimetric water content. Resulting profiles of relative density and gravimetric water content are shown in Figure 6, with target values indicated using dashed lines. Relative

densities range from 54% to 86%, relative compactions range from 87% to 97%, and gravimetric water contents range from 3.2% to 9.1%. Table 3 provides average soil properties for each GRS bridge abutment specimen and indicates that average relative density ranges from 64% to 73% and average gravimetric water content ranges from 4.3% to 6.7%, which are generally close to the corresponding target values ($D_r = 70\%$ and $w_c = 5\%$). Considering that the compaction curve is essentially flat for this sand (Zheng et al. 2018c), the variation in water content is unlikely to significantly affect the compacted dry unit weight.

Apparent cohesion for unsaturated soils can have a significant effect on soil shear modulus (Khosravi et al. 2010) and the stability of GRS walls (Vahedifard et al. 2014, 2015). The gravimetric water content profile in Figure 6(b) can be combined with the SWRCs in Figure 4 to calculate a range of apparent cohesion c'_a as (Lu et al. 2010):

$$c'_a = \sigma^s \tan \phi' = S_e s \tan \phi' \quad (2)$$

where σ^s = suction stress, $S_e = (\theta - \theta_r) / (\theta_{\max} - \theta_r)$ = effective saturation, and θ is calculated from Equation (1). For the abutment specimens, matric suction ranges from 3 kPa to 10 kPa and corresponding values of apparent cohesion are relatively uniform with elevation and have an average of 2 kPa.

Instrumentation

Instrumentation for the abutment specimens included string potentiometers, linear potentiometers, accelerometers, total pressure cells, strain gauges, and load cells. Figure 7 shows typical instrumentation layouts for the longitudinal centerline section L1, located at distance $y = 0.8$ m from the west side wall facing, longitudinal off-centerline section L2, located at $y = 0.35$ m, and transverse section T1 under the bridge seat, located at distance $x = 0.48$ m from the front

227 wall facing, as indicated in Figure 2(a). Horizontal displacements for the front wall facing blocks
228 were measured using string potentiometers and horizontal displacements for the west side wall
229 facing blocks were measured using linear potentiometers. String potentiometers were used to
230 measure settlements at the four corners of the bridge seat (Figure 2a). Accelerometers were
231 attached to the facing blocks, placed within the backfill soil, and attached to structural components
232 to measure horizontal accelerations in the longitudinal direction. Earth pressure cells were placed
233 in the backfill soil to measure vertical and lateral total stresses. Reinforcement tensile strains were
234 measured using strain gauges mounted in pairs at the mid-point of longitudinal ribs of the geogrid,
235 with one gauge mounted on top and the other on the bottom to correct for bending (Runser et al.
236 2001; Bathurst et al. 2002). Tensile strains were measured along five geogrid layers for section L1
237 (Figure 7a) and three geogrid layers for section L2 (Figure 7b) in Specimens 1, 2, and 4, and were
238 measured along seven layers for section L1 and one layer at mid-height for section L2 in Specimen
239 3. All measured geogrid strains were adjusted using a correction factor (CF), defined as the ratio
240 of global strain to gauge strain. Based on laboratory tensile test results for the same geogrid, $CF =$
241 1.1 for the current study and is not significantly affected by strain rate (Zheng et al. 2018c).

243 **Experimental Results**

244 Experimental results are presented for three instrumented sections (L1, L2, and T1) of each
245 GRS bridge abutment specimen to evaluate static loading response during construction, including
246 wall facing displacements, bridge seat settlements, soil stresses, and reinforcement tensile strains.
247 The data from each section are evaluated after construction of the lower GRS fill (Stage 1), after
248 placement of the bridge seat and construction of the upper GRS fill (Stage 2), and after placement
249 of the bridge beam (Stage 3). Outward displacements for the front wall and side wall facings and

downward displacements (i.e., settlements) for the bridge seat are defined as positive.

Facing Displacements

Profiles of wall facing displacement for longitudinal sections L1 and L2, and transverse section T1 after the three stages of construction are shown in Figures 8 and 9, respectively, and the maximum value from each profile is presented in Figure 10. Maximum displacements for sections L1 and L2 were similar at corresponding stages of construction. The only exception is the value of maximum displacement for Specimen 4, section L1, at elevation $z = 0.975$ m, which appears to be anomalous and is not included in Figure 10. For each abutment specimen, Figure 8 shows similar profile shapes for sections L1 and L2, with maximum displacements measured near the mid-height of the wall for Stages 1 and 2 and near the top for Stage 3. Facing displacements increased slightly due to placement of the bridge seat and construction of the upper GRS fill (Stage 2), and increased more significantly due to placement of the bridge beam (Stage 3). For Stage 3, Specimen 1 experienced larger displacements in the upper section of the wall than Specimen 2 due to the higher applied surcharge stress. The data also show that, compared to the baseline case (Specimen 1), facing displacements generally increased with larger reinforcement vertical spacing (Specimen 3) and reduced reinforcement tensile stiffness (Specimen 4). This finding is consistent with numerical simulation results reported by Helwany et al. (2007), Ambauen et al. (2015), Zheng and Fox (2016, 2017), and Zheng et al. (2018a).

Corresponding profiles of wall facing displacement for transverse section T1 are shown in Figure 9. Although the specimen configuration in Specimens 1 and 2 was the same for Stages 1 and 2, displacements in Specimen 2 were larger than those in Specimen 1. This may be attributed to greater compaction of the backfill soil near the side walls for Specimen 2. Similar to Figure 8,

facing displacements for section T1 in Specimens 3 and 4 were larger than in Specimen 1 after placement of the bridge beam (Stage 3) due to the effects of larger reinforcement vertical spacing and reduced reinforcement tensile stiffness, respectively.

Total facing displacements, as presented in Figures 8 to 10, may reflect unintended variations during construction and instrumentation of the GRS bridge abutment specimens. To eliminate these effects, incremental facing displacements due to placement of the bridge beam (i.e., from Stage 2 to Stage 3) are plotted in Figure 11 for all three sections. The incremental displacement profiles show better consistency and provide clearer information than the total displacement profiles. In Figure 11(a) for the front wall and section L1, the profiles show consistent trends for the four specimens, with displacements increasing with elevation and maximum values measured near the top of the wall. Incremental displacements for the upper section of the wall in Specimen 1 were larger than those in Specimen 2 due to the higher applied surcharge stress. Incremental displacements for Specimen 4 were substantially larger than for Specimen 1, and were consistently the largest for Specimen 3, with a maximum value of 2.0 mm at $z = 1.575$ m. Figure 11(b) shows similar trends for longitudinal section L2 with a maximum value of 2.8 mm for Specimen 3. For the west side wall and section T1, Figure 11(c) also indicates similar trends and generally smaller values with a maximum of 1.3 mm for Specimen 3. Figure 11 shows that incremental facing displacements increased with higher surcharge stress and were consistently larger for Specimen 3 than for Specimen 4. Thus, for the conditions tested, larger reinforcement vertical spacing had a greater effect on facing displacements than reduced reinforcement tensile stiffness.

Bridge Seat Settlements

Time histories of the settlements measured at the four top corners of the bridge seat during placement of the bridge beam (Stage 3) for Specimen 1, along with the average settlement, are presented in Figure 12. The string potentiometer on the southeast (SE) side of the bridge seat malfunctioned for this stage and was replaced prior to the shaking table tests described in the companion paper (Zheng et al. 2019). Bridge seat settlements occurred immediately on placement of the bridge beam and experienced a small amount of creep with time. After 92 hours, the average settlement on the west side of the bridge seat (NW and SW) was 3.1 mm, and the settlement on the east (NE) was 0.7 mm. This indicates tilting of the bridge seat toward the west side due to placement of the bridge beam. The final average bridge seat settlement was 2.3 mm based on the three measurements, which corresponds to a vertical strain of 0.11% for the 2.1 m-high lower GRS fill.

Final values of average bridge seat settlement due to placement of the bridge beam for each GRS bridge abutment specimen are provided in Table 4. Specimen 2 yielded the smallest settlement (1.5 mm) due to the lower applied surcharge stress. Interestingly, the ratio of settlement for Specimens 2 and 1 ($1.5 \text{ mm}/2.3 \text{ mm} = 0.652$) is equal to the ratio of applied stress ($43 \text{ kPa}/66 \text{ kPa} = 0.652$), which indicates a linear relationship between bridge seat settlement and applied surcharge stress of 0.035 mm/kPa for these working stress conditions. This linearity would not be expected to hold for higher applied surcharge stress conditions approaching failure (Zheng et al. 2018a). The bridge seat for Specimen 3 experienced the largest average settlement (3.5 mm) due to the larger reinforcement vertical spacing. The ratio of settlement in this case ($3.5 \text{ mm}/2.3 \text{ mm} = 1.52$) is not proportional to the spacing ratio of 2.0, and suggests that the backfill soil carried a greater fraction of the applied stress for Specimen 3 as compared to Specimen 1. The average

settlement of the bridge seat for Specimen 4 (2.4 mm) was only slightly larger than for Specimen 1 (2.3 mm), which indicates that reduced reinforcement tensile stiffness had only a small effect on bridge seat settlement for the current study.

Soil Stresses

Profiles of vertical soil stress behind the front wall facing for longitudinal centerline section L1 after Stage 1 and Stage 3 are shown in Figure 13 for the four abutment specimens. Vertical stress profiles obtained from the AASHTO (2012) method also are shown for comparison, in which values for Stage 1 were calculated using soil self-weight and values for Stage 3 were calculated using soil self-weight plus a fraction of the applied surcharge stress from a 2:1 stress distribution. Figure 13(a) shows that measured vertical stresses for Stage 1 increased with depth and were similar for the four specimens. The measurements are in close agreement with AASHTO (2012) calculated values near the top of the fill and progressively diverge toward lower values at the bottom. The difference is attributed to friction developed at the back of facing blocks and partial support of backfill soil weight from reinforcement near the facing, similar to the findings of Runser et al. (2001).

Measured vertical stress profiles for Stage 3, after placement of the bridge beam, are shown in Figure 13(b). Values are similar at lower elevations and then diverge significantly near the top. The highest value (70.1 kPa, $z = 1.875$ m) was measured for Specimen 1 and is nearly equal to the applied surcharge stress (66 kPa) plus the small additional vertical stress (3.9 kPa) due to the thin (0.225 m) layer of cover soil. Values at the top for Specimens 3 and 4 were lower than for Specimen 2, even though the applied surcharge stress for Specimens 3 and 4 (66 kPa) was higher than for Specimen 2 (43 kPa). The discrepancies in measured vertical stress near the top are

342 attributed to variability in placement of pressure cells and bridge seats during construction and
343 irregularities in contact stress between the bridge seats and backfill soil (McCartney et al. 2018).
344 Measured vertical stresses for Stage 3 were generally larger than AASHTO (2012) values for Stage
345 1 and smaller than AASHTO (2012) values for Stage 3, with the exception of Specimen 1 at the
346 top. The assumed 2:1 stress distribution used in the AASHTO (2012) method is a first
347 approximation and does not account for lateral distance from the wall facing, which affects the
348 stress state near the top of the lower GRS fill for the abutment specimens.

349 Corresponding profiles of measured and calculated lateral soil stress behind the front wall
350 facing are shown in Figure 14. To obtain the AASHTO (2012) calculated values, the AASHTO
351 (2012) vertical stress profiles in Figure 13 were multiplied by the Rankine active earth pressure
352 coefficient K_a ($= 0.12$). In Figure 14(a), measured lateral stresses for Stage 1 were smaller than
353 5 kPa and show a general but inconsistent trend of increasing magnitude with depth. Measured
354 lateral stresses near the top of the wall were larger than the AASHTO (2012) values, which is
355 attributed to the effects of soil compaction, and smaller than the AASHTO (2012) values near the
356 bottom, which is attributed to reduced vertical stress in Figure 13(a). For Stage 3 in Figure 14(b),
357 measured lateral stresses increased near the top of the wall due to placement of the bridge beam
358 and generally were larger at top and bottom than at mid-height, which is similar to the trend of
359 AASHTO (2012) calculated lateral stress profiles. All measured lateral stresses behind the wall
360 facing were smaller than AASHTO (2012) calculated values, and thus indicates that the AASHTO
361 (2012) lateral stress profiles for Stage 3 static loading are conservative for this study.

Reinforcement Strains

Distributions of measured reinforcement tensile strain for the three instrumented sections of Specimen 1 are shown in Figure 15. Zero strain at the free end of each reinforcement layer is also plotted. For longitudinal section L1 and Stage 1, maximum tensile strains occurred near the facing block connections in layers 1, 4, and 7, and at a distance of $x = 0.8$ m from the facing in layer 10. Tensile strains in layer 13 were small and do not indicate a clear maximum. Strains increased slightly due to placement of the bridge seat and construction of the upper GRS fill (Stage 2), and then increased substantially due to placement of the bridge beam (Stage 3). For Stage 3, the maximum tensile strain occurred near the facing connections in lower layers 1, 4, and 7, and under the bridge seat in upper layers 10 and 13.

Reinforcement tensile strains for longitudinal section L2 are shown in Figure 15(b) and display similar magnitudes and trends for Stages 1 and 2. For Stage 3, tensile strains were similar to the L1 values in layers 1 and 7 and much larger than the L1 values in layer 13 under the bridge seat. This is attributed to tilting of the bridge seat toward the west side of the abutment (i.e., section L2) for Stage 3, as indicated in Figure 12. Reinforcement tensile strains for transverse section T1 are shown in Figure 15(c). Similar to the observations for sections L1 and L2, the maximum tensile strain in each reinforcement layer for Stage 1 occurred near the facing connection in layers 1 and 7, and the strains were generally small in layer 13. For Stage 3, the application of surcharge stress caused a significant increase in tensile strain for layers 7 and 13. Interestingly, the two points of maximum strain for the uppermost reinforcement layers in sections T1 and L2 (i.e., 0.14% at $x = 0.48$ m, $y = 0.33$ m, $z = 1.98$ m for T1, and 0.15% at $x = 0.45$ m, $y = 0.35$ m, $z = 1.95$ m for L2), were nearly co-located within Specimen 1 and indicate essentially the same tensile strain values in both longitudinal and transverse directions.

Similar to Figure 11, plots of incremental strain provide clearer information. Distributions of incremental reinforcement tensile strain due to placement of the bridge beam (i.e., from Stage 2 to Stage 3) for longitudinal section L1 are shown in Figure 16(a) for the four abutment specimens. The trends are consistent with previous plots. The effect of applied surcharge stress was most clearly observed for layer 7, in which incremental strains for Specimen 1 were larger than for Specimen 2 near the wall facing, and incremental strains for Specimen 4 were larger than for Specimen 1 and largest for Specimen 3. For the conditions tested, larger reinforcement vertical spacing had a more significant effect than reduced reinforcement tensile stiffness. Similar trends are observed for section T1, as shown in Figure 16(b).

Conclusions

This paper presents experimental results from physical model tests on four half-scale geosynthetic reinforced soil (GRS) bridge abutment specimens constructed using well-graded backfill sand, modular facing blocks, and uniaxial geogrid reinforcement for working stress, static loading conditions. The specimens included a baseline case (Specimen 1), lower surcharge stress (Specimen 2), larger reinforcement vertical spacing (Specimen 3), and reduced reinforcement tensile stiffness (Specimen 4). Results are presented after construction of the lower GRS fill (Stage 1), after placement of the bridge seat and construction of the upper GRS fill (Stage 2), and after placement of the bridge beam (Stage 3). The following conclusions are reached for the conditions of the study:

1. The abutment specimens experienced similar profiles of wall facing displacement, with maximum displacements measured near the mid-height for Stages 1 and 2 and near the top for Stage 3. For the front wall and Stage 3 loading, incremental displacements increased

with elevation along the wall, higher surcharge stress, reduced reinforcement tensile stiffness, and larger reinforcement vertical spacing. Corresponding incremental facing displacements for the west side wall were smaller in magnitude and showed similar trends.

2. Bridge seat settlements occurred immediately on placement of the bridge beam and experienced a small amount of creep with time. Settlement was proportional to the applied surcharge stress, strongly affected by larger reinforcement vertical spacing, and only slightly affected by reduced reinforcement tensile stiffness.

3. Measured vertical and lateral soil stresses behind the wall facing generally were lower than values calculated using the AASHTO (2012) method for Stage 1 and Stage 3. Lateral soil stresses increased near the top of the wall due to placement of the bridge beam, and were larger at top and bottom sections of the wall than at mid-height.

4. Tensile strains increased significantly in the higher reinforcement layers during Stage 3 loading. The maximum tensile strain occurred near the facing block connection for lower reinforcement layers and under the bridge seat for higher layers in both longitudinal and transverse sections. Incremental reinforcement tensile strains due to placement of the bridge beam increased with larger reinforcement vertical spacing and reduced reinforcement tensile stiffness.

Acknowledgements

Financial support for this study provided by the California Department of Transportation (Caltrans) Project 65A0556 with Federal Highway Administration (FHWA) Pooled Fund Project 1892AEA is gratefully acknowledged. The authors thank Dr. Charles Sikorsky and Kathryn Griswell of Caltrans for their support and assistance with the project. The first author gratefully

acknowledges a GSI Fellowship provided by the Geosynthetic Institute. The authors also thank the staff and undergraduate research assistants at the UCSD Powell Structural Laboratories for their help with the experimental work. The geogrid used in this study was provided by the Tensar International Corporation, Inc.

Notation

The following symbols are used in this paper:

c'_a = apparent cohesion

C_c = compression index

C_r = recompression index

C_u = coefficient of uniformity

C_z = coefficient of curvature

D_{50} = mean particle size

D_r = relative density

e_o = initial void ratio

e_{\max} = maximum void ratio

e_{\min} = minimum void ratio

G_s = specific gravity of solids

h = height of lower GRS fill

$J_{5\%}$ = secant stiffness of reinforcement at 5% tensile strain

J_i = tensile stiffness of the i^{th} reinforcement layer in the longitudinal direction

- 455 K_a = Rankine coefficient of active earth pressure
- 456 n = number of reinforcement layers in the longitudinal direction
- 457 N_{vG} = van Genuchten (1980) SWRC model parameter
- 458 s = matric suction
- 459 S_e = effective saturation
- 460 S_v = reinforcement vertical spacing
- 461 T_{ult} = ultimate strength of reinforcement
- 462 w_c = gravimetric water content
- 463 x = distance from front wall facing
- 464 y = distance from west side wall facing
- 465 z = elevation above foundation soil
- 466 α_{vG} = van Genuchten (1980) SWRC model parameter
- 467 γ_d = dry unit weight
- 468 ϕ'_p = peak friction angle
- 469 σ'_3 = minor principal effective stress
- 470 σ^s = suction stress
- 471 θ = volumetric water content
- 472 θ_d = drying curve volumetric water content at zero suction
- 473 θ_{max} = volumetric water content at zero matric suction
- 474 θ_r = residual volumetric water content
- 475 θ_w = wetting curve volumetric water content at zero suction

ψ = dilation angle

References

- AASHTO. (2012). *AASHTO LRFD bridge design specifications*, 6th Edition, American Association of State Highway and Transportation Officials, Washington, D.C.
- Abu-Farsakh, M., Ardah, A., and Voyiadjis, G. (2018). "3D finite element analysis of the geosynthetic reinforced soil-integrated bridge system (GRS-IBS) under different loading condition." *Transportation Geotechnics*, 15, 70-83.
- Abu-Hejleh, N., Zornberg, J.G., Wang, T., and Watcharamonthein, J. (2002). "Monitored displacements of unique geosynthetic-reinforced soil bridge abutments." *Geosynthetics International*, 9(1), 71-95.
- Adams, M. (1997). "Performance of a prestrained geosynthetic reinforced soil bridge pier." *Mechanically Stabilized Backfill*, Balkema, Rotterdam, Netherlands, 35-53.
- Adams, M., Nicks, J., Stabile, T., Wu, J., Schlatter, W., and Hartmann, J. (2011a). "Geosynthetic reinforced soil integrated bridge system synthesis report." *FHWA-HRT-11-027*, U.S. DOT, Washington, D.C.
- Adams, M., Nicks, J., Stabile, T., Wu, J., Schlatter, W., and Hartmann, J. (2011b). "Geosynthetic reinforced soil integrated bridge system interim implementation guide." *FHWA-HRT-11-026*, U.S. DOT, Washington, D.C.
- Adams, M.T., Ooi, P.S., and Nicks, J.E. (2014). "Mini-pier testing to estimate performance of full-scale geosynthetic reinforced soil bridge abutments." *Geotechnical Testing Journal*, 37(5), 884-894.

- Allen, T.M., and Bathurst, R.J. (2014a). "Design and performance of 6.3-m-high, block-faced geogrid wall designed using K-stiffness method." *Journal of Geotechnical and Geoenvironmental Engineering*, 142(2), 04013016.
- Allen, T.M., and Bathurst, R.J. (2014b). "Performance of an 11 m high block-faced geogrid wall designed using the K-stiffness method." *Canadian Geotechnical Journal*, 51(1), 16-29.
- Ambauen, S., Leshchinsky, B., Xie, Y., and Rayamajhi, D. (2015). "Service-state behavior of reinforced soil walls supporting spread footings: a parametric study using finite-element analysis." *Geosynthetics International*, 23(3), 156-170.
- Ardah, A., Abu-Farsakh, M., and Voyiadjis, G. (2017). "Numerical evaluation of the performance of a Geosynthetic Reinforced Soil-Integrated Bridge System (GRS-IBS) under different loading conditions." *Geotextiles and Geomembranes*, 45(6), 558-569.
- ASTM D6637-15, *Standard Test Method for Determining Tensile Properties of Geogrids by the Single or Multi-Rib Tensile Method*, ASTM International.
- Bathurst, R.J., Allen, T.M., and Walters, D.L. (2002). "Short-term strain and deformation behavior of geosynthetic walls at working stress conditions." *Geosynthetics International*, 9(5-6), 451-482.
- Bathurst, R.J., Vlachopoulos, N., Walters, D.L., Burgess, P.G., and Allen, T.M. (2006). "The influence of facing stiffness on the performance of two geosynthetic reinforced soil retaining walls." *Canadian Geotechnical Journal*, 43(12), 1225-1237.
- Bathurst, R.J., Nernheim, A., Walters, D.L., Allen, T.M., Burgess, P., and Saunders, D.D. (2009). "Influence of reinforcement tensile stiffness and compaction on the performance of four geosynthetic reinforced soil walls." *Geosynthetics International*, 16(1), 43-59.

- Budge, A.S., Dasenbrock, D.D., Mattison, D.J., Bryant, G.K., Grosser, A.T., Adams, M., and Nicks, J. (2014). "Instrumentation and early performance of a large grade GRS-IBS wall." *Geo-Congress 2014*, ASCE, Reston, VA, USA, 4213-4227.
- Ehrlich, M., and Mirmoradi, S.H. (2013). "Evaluation of the effects of facing stiffness and toe resistance on the behavior of GRS walls." *Geotextiles and Geomembranes*, 40, 28-36.
- Ehrlich, M., Mirmoradi, S.H., and Saramago, R.P. (2012). "Evaluation of the effect of compaction on the behavior of geosynthetic-reinforced soil walls." *Geotextiles and Geomembranes*, 34, 108-115.
- Gotteland, P., Gourc, J.P., and Villard, P. (1997). "Geosynthetic reinforced structures as bridge abutments: Full scale experimentation and comparison with modelisations." *Mechanically Stabilized Backfill*, Balkema, Rotterdam, Netherlands, 25-34.
- Helwany, S.M.B., Wu, J.T.H., and Froessl, B. (2003). "GRS bridge abutments – An effective means to alleviate bridge approach settlement." *Geotextiles and Geomembranes*, 21(3), 177-196.
- Helwany, S.M.B., Wu, J.T.H., and Kitsabunnarat, A. (2007). "Simulating the behavior of GRS bridge abutments." *Journal of Geotechnical and Geoenvironmental Engineering*, 133(10), 1229-1240.
- Helwany, S.M.B., Wu, J.T.H., and Meinholz, P. (2012). "Seismic design of geosynthetic-reinforced soil bridge abutments with modular block facing." *NCHRP Web-Only Document 187*, Transportation Research Board, Washington, D.C.
- Iwamoto, M.K., Ooi, P.S., Adams, M.T., and Nicks, J.E. (2015). "Composite properties from instrumented load tests on mini-piers reinforced with geotextiles." *Geotechnical Testing Journal*, 38(4), 397-408.

- Jiang, Y., Han, J., Parsons, R.L., and Brennan, J. (2016). "Field instrumentation and evaluation of modular-block MSE walls with secondary geogrid layers." *Journal of Geotechnical and Geoenvironmental Engineering*, 142(12), 05016002.
- Ketchart, K., and Wu, J.T.H. (1997). "Performance of geosynthetic-reinforced soil bridge pier and abutment, Denver, Colorado, USA." *Mechanically Stabilized Backfill*, Balkema, Rotterdam, Netherlands, 101-116.
- Khosravi, A., Ghayoomi, M., McCartney, J.S., and Ko, H.-Y. (2010). "Impact of effective stress on the dynamic shear modulus of unsaturated sands." *GeoFlorida 2010: Advances in Analysis, Modeling & Design*, ASCE, Reston, VA, USA, 410-419.
- Lee, K.Z.Z., and Wu, J.T.H. (2004). "A synthesis of case histories on GRS bridge-supporting structures with flexible facing." *Geotextiles and Geomembranes*, 22(4), 181-204.
- Leshchinsky, B., and Xie, Y. (2015). "MSE walls as bridge abutments: Optimal reinforcement density." *Geotextiles and Geomembranes*, 43(2), 128-138.
- Lu, N., Godt, J.W., and Wu, D.T. (2010). "A closed-form equation for effective stress in unsaturated soil." *Water Resources Research*, Vol. 46, W05515, 10.1029/2009WR008646.
- McCartney, J.S., Shing, P.B., Zheng, Y., Rong, W., and Fox, P.J. (2018). "Interaction of MSE abutments with bridge superstructures under seismic loading – shaking table tests." *Report No. SSRP 18-01*, California Department of Transportation (Caltrans), Sacramento, CA, USA.
- Mirmoradi, S.H., and Ehrlich, M., (2017). "Effects of facing, reinforcement tensile stiffness, toe resistance, and height on reinforced walls." *Geotextiles and Geomembranes*, 45(1), 67-76.
- Nicks, J.E., Adams, M.T., Ooi, P.S.K., and Stabile, T. (2013). "Geosynthetic reinforced soil performance testing – axial load deformation relationships." *FHWA-HRT-13-066*, U.S. DOT, Washington, D.C.

- Nicks, J.E., Esmaili, D., and Adams, M.T. (2016). "Deformations of geosynthetic reinforced soil under bridge service loads." *Geotextiles and Geomembranes*, 44(4), 641-653.
- Rong, W., Zheng, Y., McCartney, J.S., and Fox, P.J. (2017). "3D deformation behavior of geosynthetic reinforced soil bridge abutments." *Geotechnical Frontiers 2017*, ASCE, Reston, VA, USA, 44-53.
- Runser, D., Fox, P. J., and Bourdeau, P.L. (2001). "Field performance of a 17 m-high reinforced soil retaining wall." *Geosynthetics International*, 8(5), 367-391.
- Saghebfar, M., Abu-Farsakh, M., Ardah, A., and Chen, Q. (2017). "Performance monitoring of Geosynthetic Reinforced Soil Integrated Bridge System (GRS-IBS) in Louisiana." *Geotextiles and Geomembranes*, 45(2), 34-47.
- Shen, P, Han, J., Zornberg, J., Morsy, A., Leshchinsky, D., Tanyu, B.F., and Xu, C. (2019). "Two and three-dimensional numerical analyses of geosynthetic-reinforced soil (GRS) piers." *Geotextiles and Geomembranes*, 47(3), 352-368.
- Trautner, C.A., Zheng, Y., McCartney, J.S., Hutchinson, T.C. (2017). "An approach for shake table performance evaluation during repair and retrofit actions." *Earthquake Engineering and Structural Dynamics*, 47(1), 131-146.
- Vahedifard, F., Leshchinsky, B., Sehat, S., and Leshchinsky, D. (2014). "Impact of cohesion on seismic design of geosynthetic-reinforced earth structures." *Journal of Geotechnical and Geoenvironmental Engineering*, 140(6), 04014016.
- Vahedifard, F., Leshchinsky, B., Mortezaei, K., and Lu, N. (2015). "Active earth pressures for unsaturated retaining structures." *Journal of Geotechnical and Geoenvironmental Engineering*, 141(11), 04015048.

- van Genuchten, M.T., 1980, "A Closed-Form Equation for Predicting the Hydraulic Conductivity of Unsaturated Soils." *Soil Science Society of America Journal*, 44(5), 892–898.
- Won, G.W., Hull, T., and De Ambrosis, L. (1996). "Performance of a geosynthetic segmental block wall structure to support bridge abutments." *Earth Reinforcement*, Vol. 1, Balkema, Rotterdam, Netherlands, 543–548.
- Wu, J.T.H., Ketchart, K., and Adams, M. (2001). "GRS bridge piers and abutments." *Report No. FHWA-RD-00-038*, U.S. DOT, Washington, D.C.
- Wu, J.T.H., Lee, K.Z.Z., Helwany, S.B., and Ketchart, K. (2006). "Design and construction guidelines for geosynthetic-reinforced soil bridge abutments with a flexible facing." *NCHRP Report 556*, Transportation Research Board, Washington, D.C.
- Xu, C., Liang, C, and Shen, P. (2019). "Experimental and theoretical studies on the ultimate bearing capacity of geogrid-reinforced sand." *Geotextiles and Geomembranes*, 47(3), 417-428.
- Zheng, Y. (2017). *Numerical Simulations and Shaking Table Tests of Geosynthetic Reinforced Soil Bridge Abutments*, PhD dissertation, University of California, San Diego, La Jolla, CA, USA.
- Zheng, Y., and Fox, P.J. (2016). "Numerical investigation of geosynthetic-reinforced soil bridge abutments under static loading." *Journal of Geotechnical and Geoenvironmental Engineering*, 10.1061/(ASCE)GT.1943-5606.0001452, 04016004.
- Zheng, Y., and Fox, P.J. (2017). "Numerical investigation of the geosynthetic reinforced soil-integrated bridge system under static loading." *Journal of Geotechnical and Geoenvironmental Engineering*, 10.1061/(ASCE)GT.1943-5606.0001665, 04017008.
- Zheng, Y., Fox, P.J., and McCartney, J.S. (2018a). "Numerical simulation of deformation and failure behavior of geosynthetic reinforced soil bridge abutments." *Journal of Geotechnical and Geoenvironmental Engineering*, DOI: 10.1061/(ASCE)GT.1943-5606.0001893.

- 611 Zheng, Y., Fox, P.J., and McCartney, J.S. (2018b). “Numerical simulation of deformation response
612 of geosynthetic reinforced soil mini-piers.” *Geosynthetics International*, DOI:
613 10.1680/jgein.18.00007.
- 614 Zheng, Y., Sander, A.C., Rong, W., Fox, P.J., Shing, P.B., McCartney, J.S. (2018c). “Shaking table
615 test of a half-scale geosynthetic-reinforced soil bridge abutment.” *Geotechnical Testing*
616 *Journal*, DOI: 10.1520/GTJ20160268.
- 617 Zheng, Y., McCartney, J.S., Shing, P. B., and Fox, P.J. (2018d). “Transverse shaking table test of a
618 half-scale geosynthetic reinforced soil bridge abutment.” *Geosynthetics International*, DOI:
619 10.1680/jgein.18.00019.
- 620 Zheng, Y., Fox, P.J., Shing, P.B., and McCartney, J.S. (2019) “Physical model tests of half-scale
621 geosynthetic reinforced soil bridge abutments. II: Dynamic loading.” *Journal of Geotechnical*
622 *and Geoenvironmental Engineering* (companion paper, in review).

Table 1. Experimental program.

Specimen	Variable	Average surcharge stress (kPa)	Reinforcement vertical spacing (m)	Reinforcement tensile stiffness (kN/m)	Global stiffness (kN/m) ^a
1	Baseline case	66	0.15	380	2352
2	Reduced surcharge stress	43	0.15	380	2352
3	Increased reinforcement vertical spacing	66	0.30	380	1267
4	Reduced reinforcement tensile stiffness	66	0.15	190	1176

^a defined as $\frac{1}{h} \sum_{i=1}^n J_i$, where J_i = tensile stiffness of the i^{th} reinforcement layer in the longitudinal direction, n = number of longitudinal reinforcement layers, and h = height of lower GRS fill (after Bathurst et al. 2009).

Table 2. Soil properties.

Property	Value
Specific gravity, G_s	2.61
Coefficient of uniformity, C_u	6.1
Coefficient of curvature, C_z	1.0
Mean particle size, D_{50} (mm)	0.85
Compression index, C_c	0.10
Recompression index, C_r	0.025
Maximum void ratio, e_{\max}	0.853
Minimum void ratio, e_{\min}	0.371
Peak friction angle, ϕ'_p ($^\circ$)	51.3
Dilation angle, ψ ($^\circ$)	13.0

Table 3. Average soil properties for GRS bridge abutment specimens.

Specimen	Average dry unit weight (kN/m ³)	Average relative compaction (%)	Average relative density (%)	Average gravimetric water content (%)
1	16.6	90	64	4.7
2	17.1	93	73	6.7
3	17.1	93	73	5.5
4	16.7	91	67	4.3

Table 4. Average values of bridge seat settlement due to placement of bridge beam.

Specimen	Average surcharge stress (kPa)	Average settlement (mm)	Average vertical strain of lower GRS fill (%)
1	66	2.3	0.11
2	43	1.5	0.07
3	66	3.5	0.17
4	66	2.4	0.11

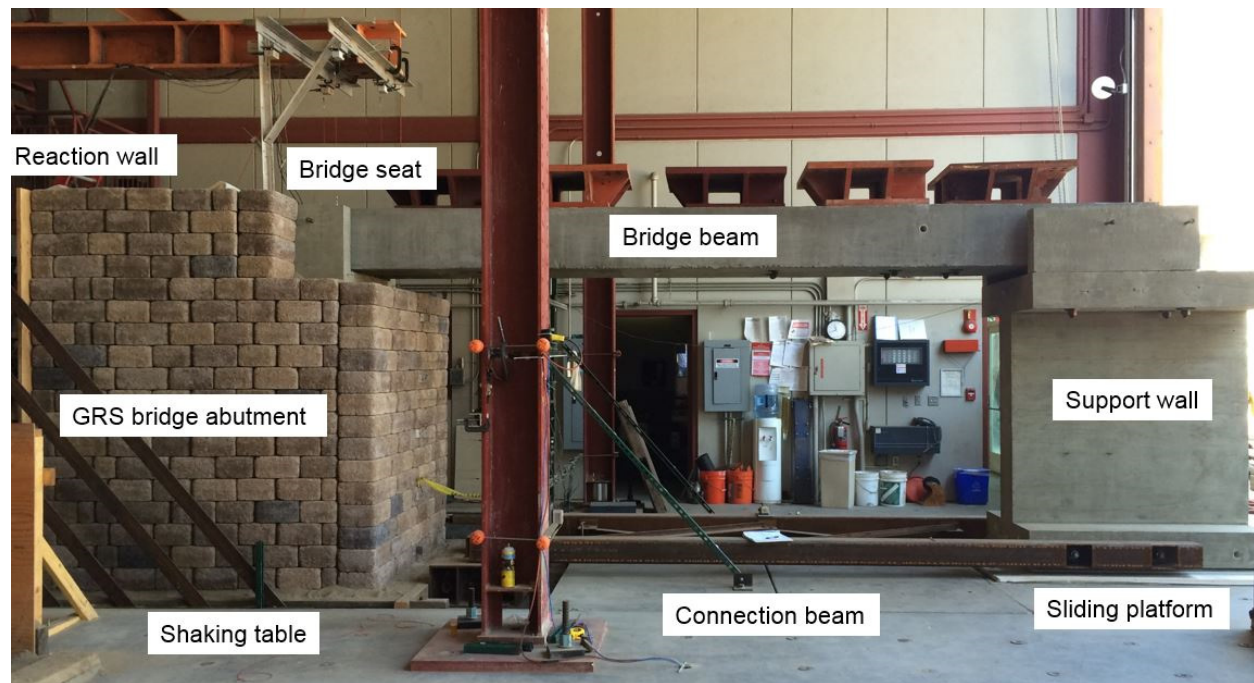


Figure 1. Configuration of GRS bridge abutment system for Specimen 1.

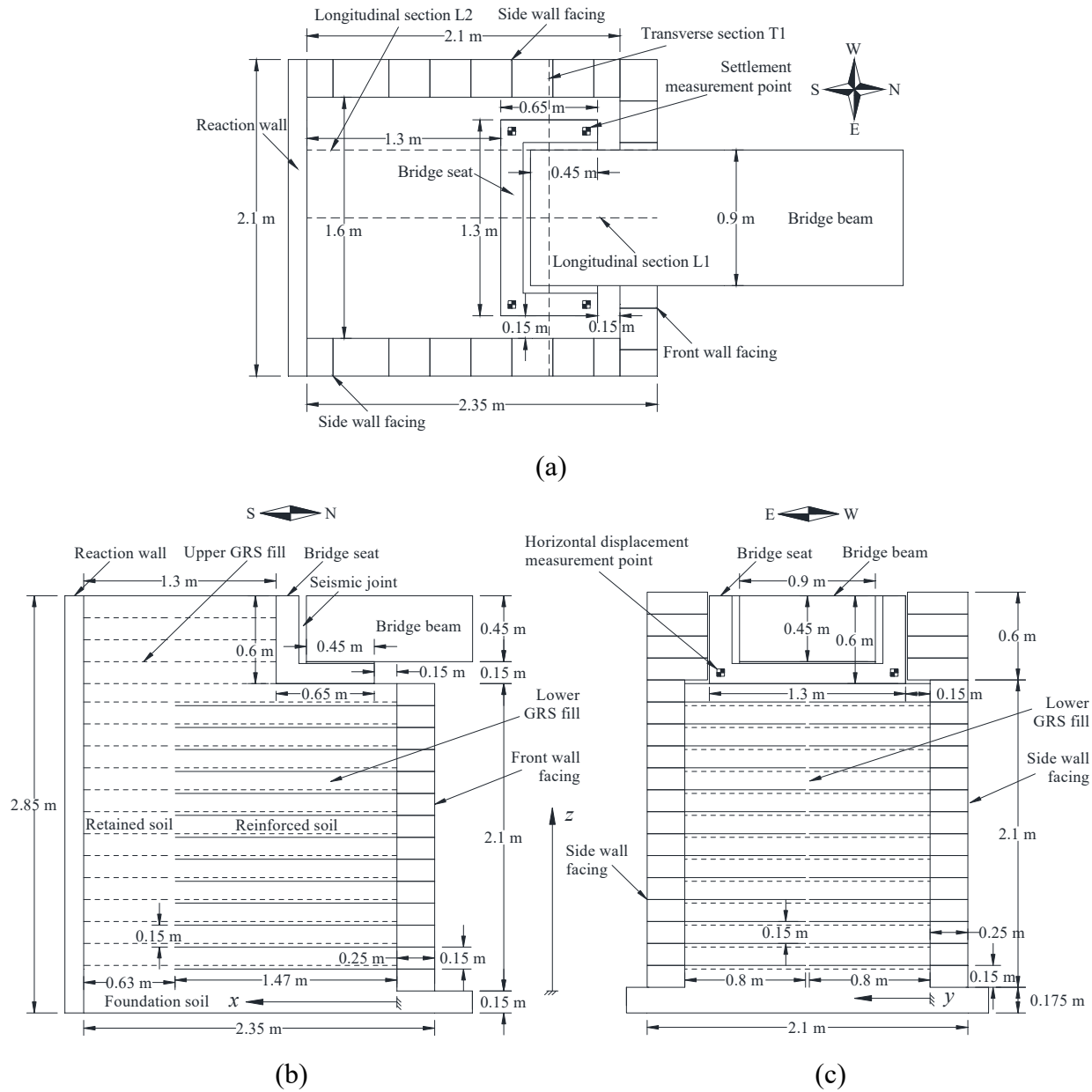
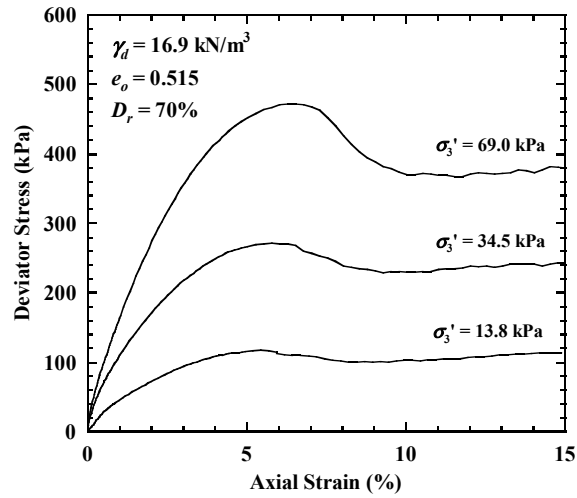
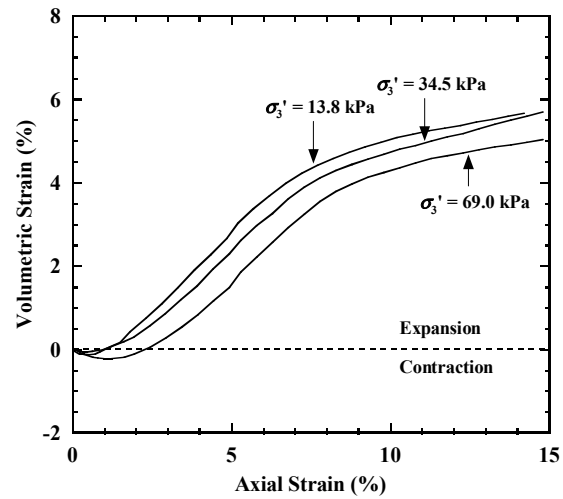


Figure 2. Specimen 1: (a) top view; (b) longitudinal cross-sectional view; (c) transverse cross-sectional view. Note: dashed lines indicate reinforcement layers perpendicular to diagram.



(a)



(b)

Figure 3. Experimental results from consolidated-drained triaxial compression tests on well-graded angular sand: (a) deviator stress; (b) volumetric strain.

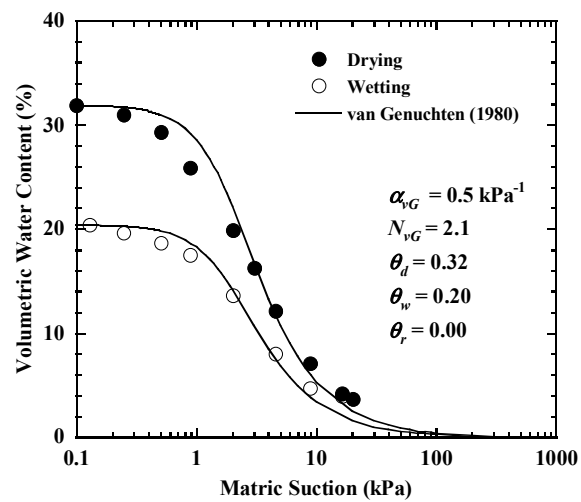


Figure 4. Wetting-path and drying-path SWRC data with fitted relationships.

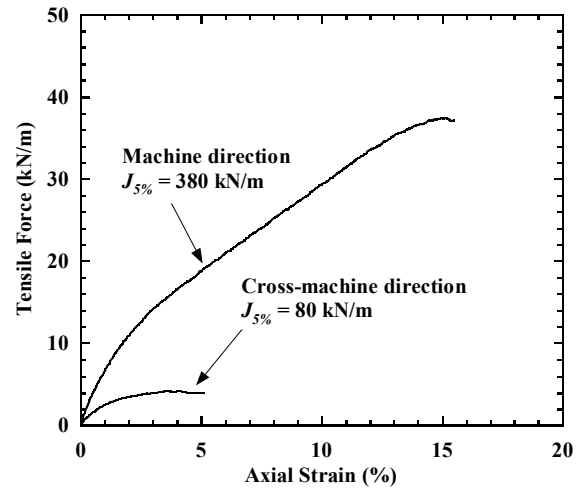
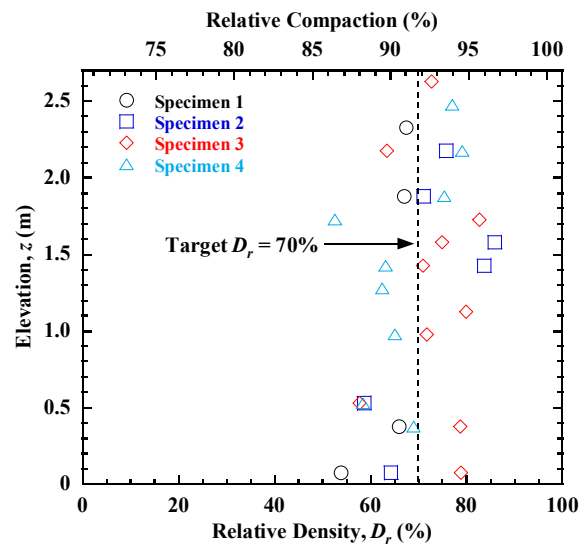
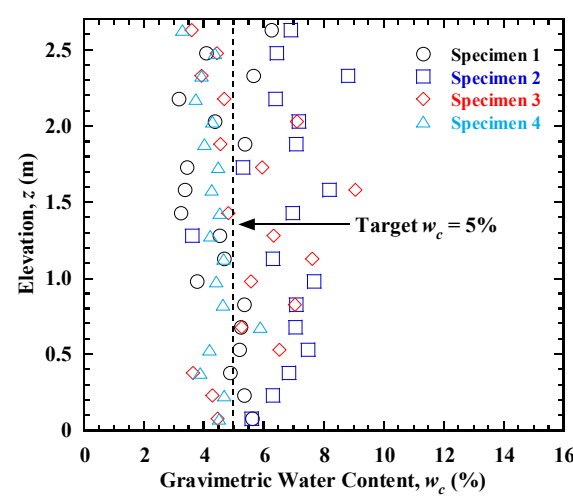


Figure 5. Experimental results from tensile tests on geogrid reinforcement.



(a)



(b)

Figure 6. Soil property profiles for GRS bridge abutment specimens: (a) relative density; (b) gravimetric water content.

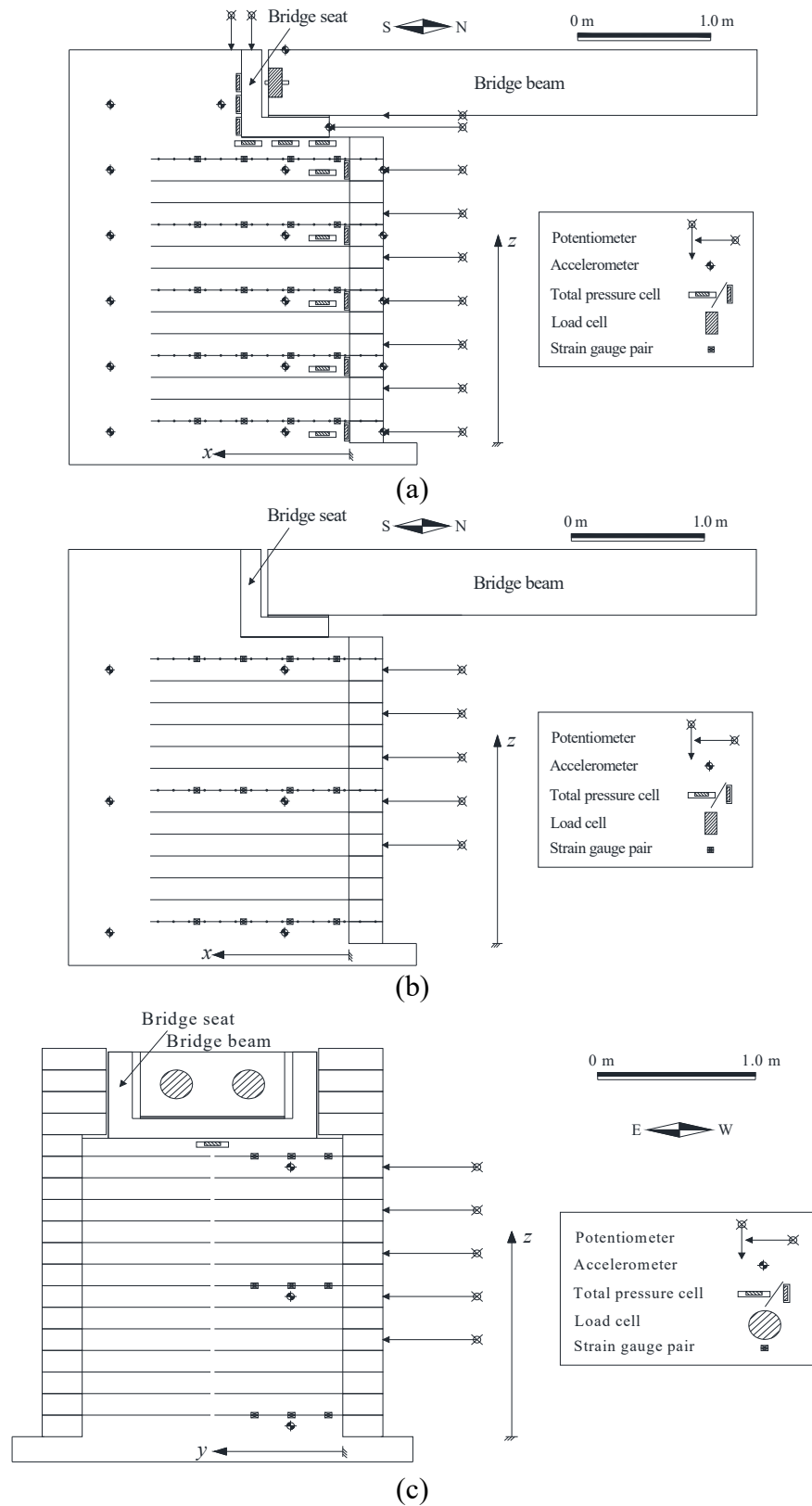


Figure 7. Instrumentation for Specimen 1: (a) longitudinal centerline section L1 ($y = 0.8$ m); (b) longitudinal off-centerline section L2 ($y = 0.35$ m); (c) transverse section T1 ($x = 0.48$ m).

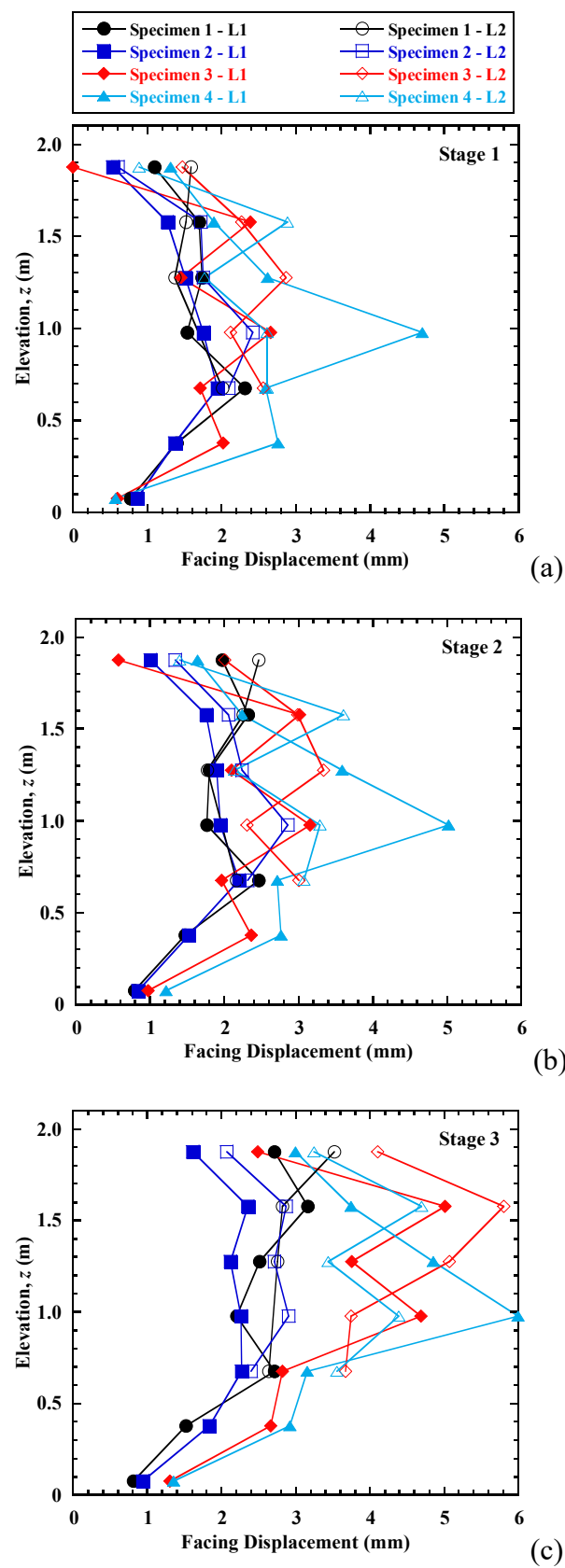


Figure 8. Profiles of facing displacement for front wall and longitudinal sections L1 and L2: (a) Stage 1; (b) Stage 2; (c) Stage 3.

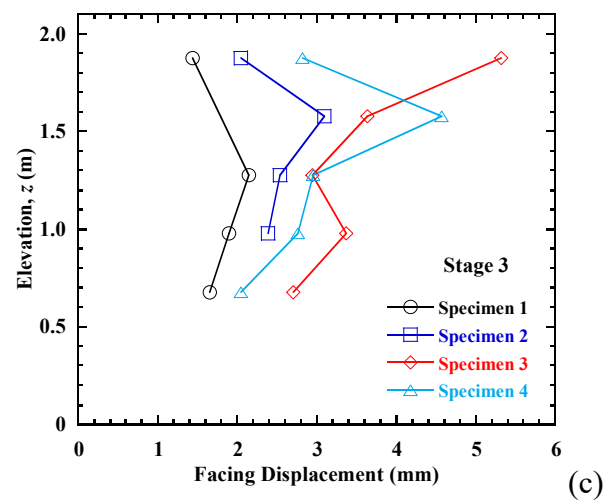
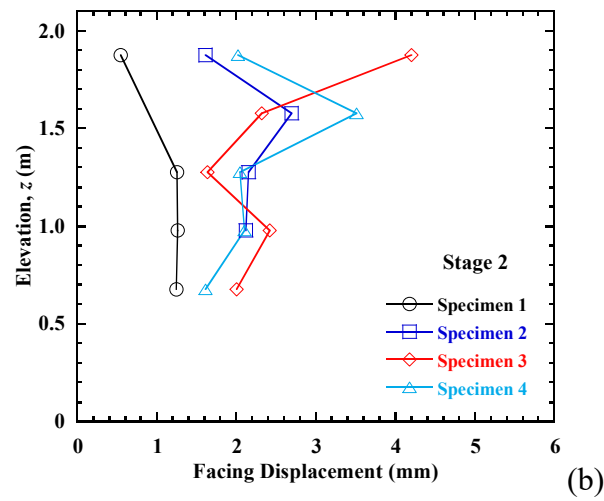
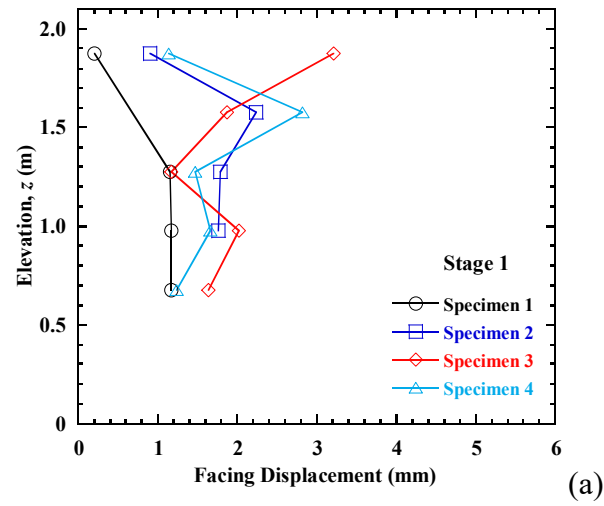


Figure 9. Profiles of facing displacement for west side wall and transverse section T1: (a) Stage 1; (b) Stage 2; (c) Stage 3.

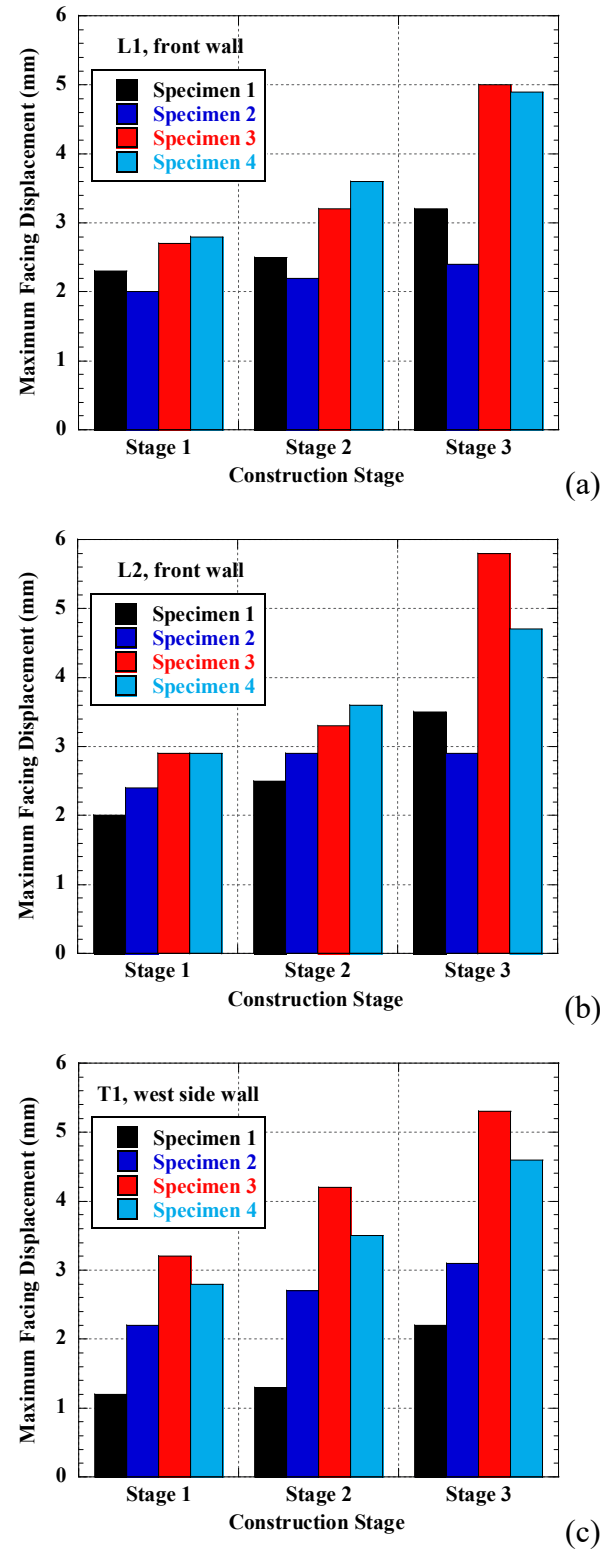


Figure 10. Maximum facing displacements: (a) L1, front wall; (b) L2, front wall; (c) T1, west side wall.

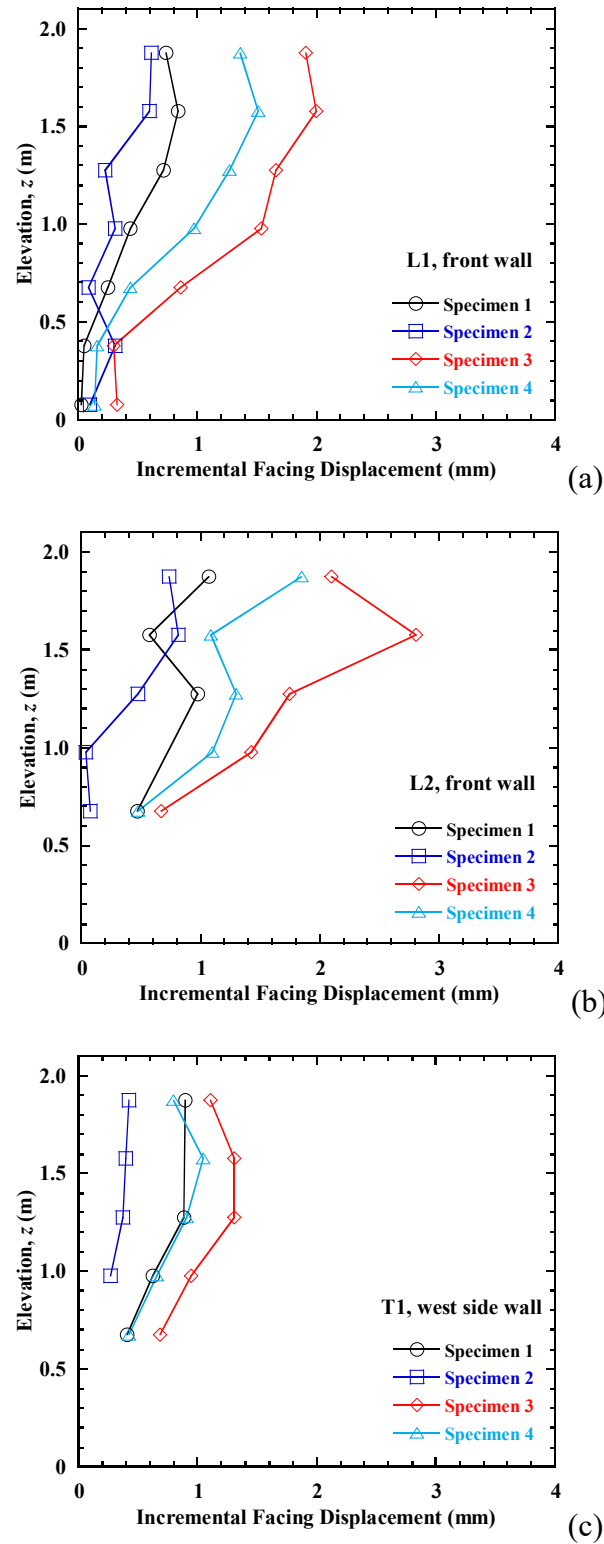


Figure 11. Profiles of incremental facing displacement due to placement of bridge beam: (a) L1, front wall; (b) L2, front wall; (c) T1, west side wall.

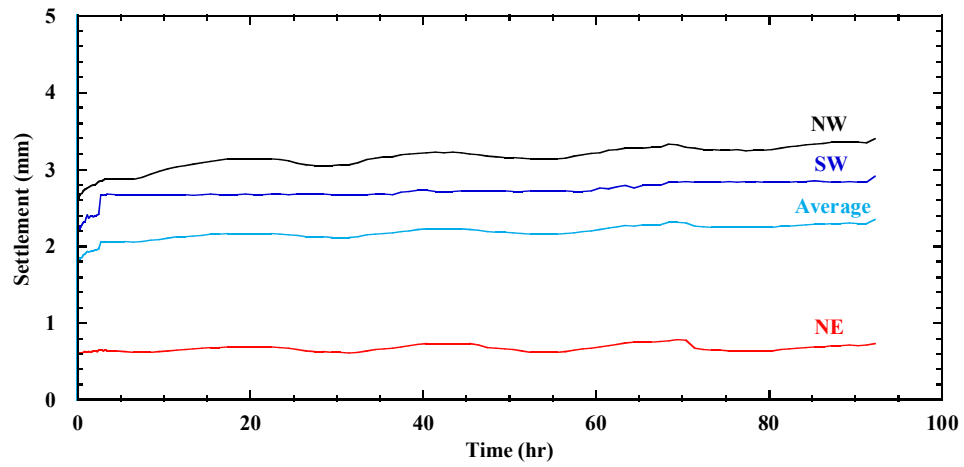
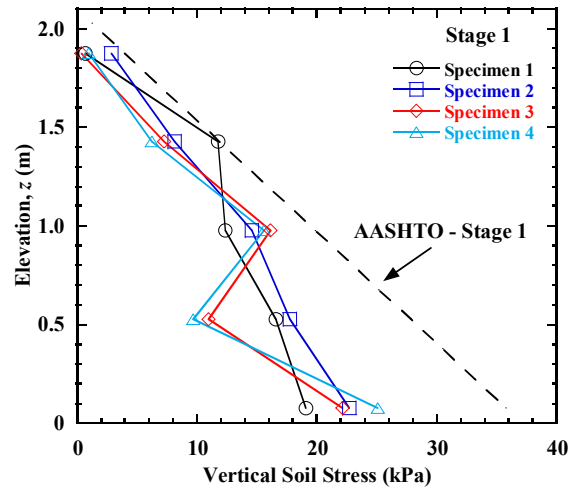
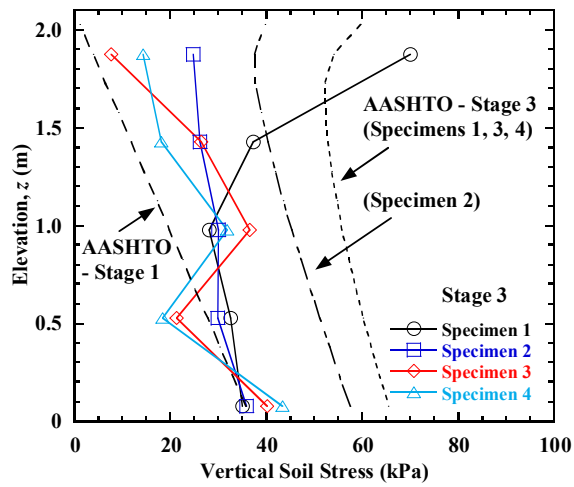


Figure 12. Time histories of settlement for bridge seat due to placement of bridge beam for Specimen 1.

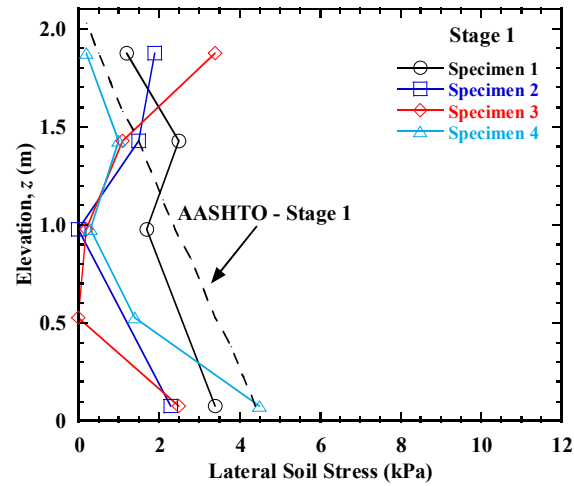


(a)

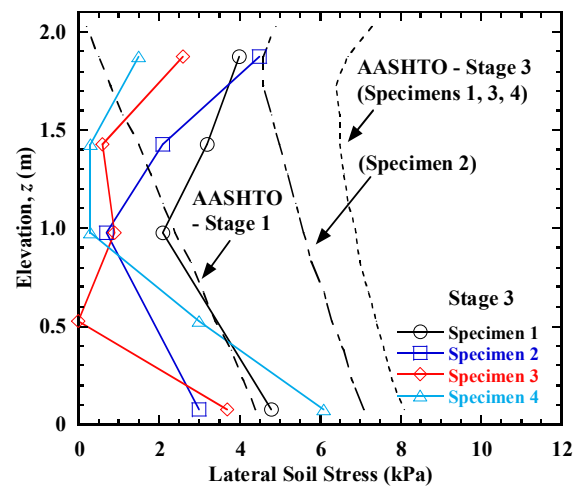


(b)

Figure 13. Profiles of vertical soil stress near front wall facing for longitudinal section L1: (a) Stage 1; (b) Stage 3.



(a)



(b)

Figure 14. Profiles of lateral soil stress behind front wall facing for longitudinal section L1: (a) Stage 1; (b) Stage 3.

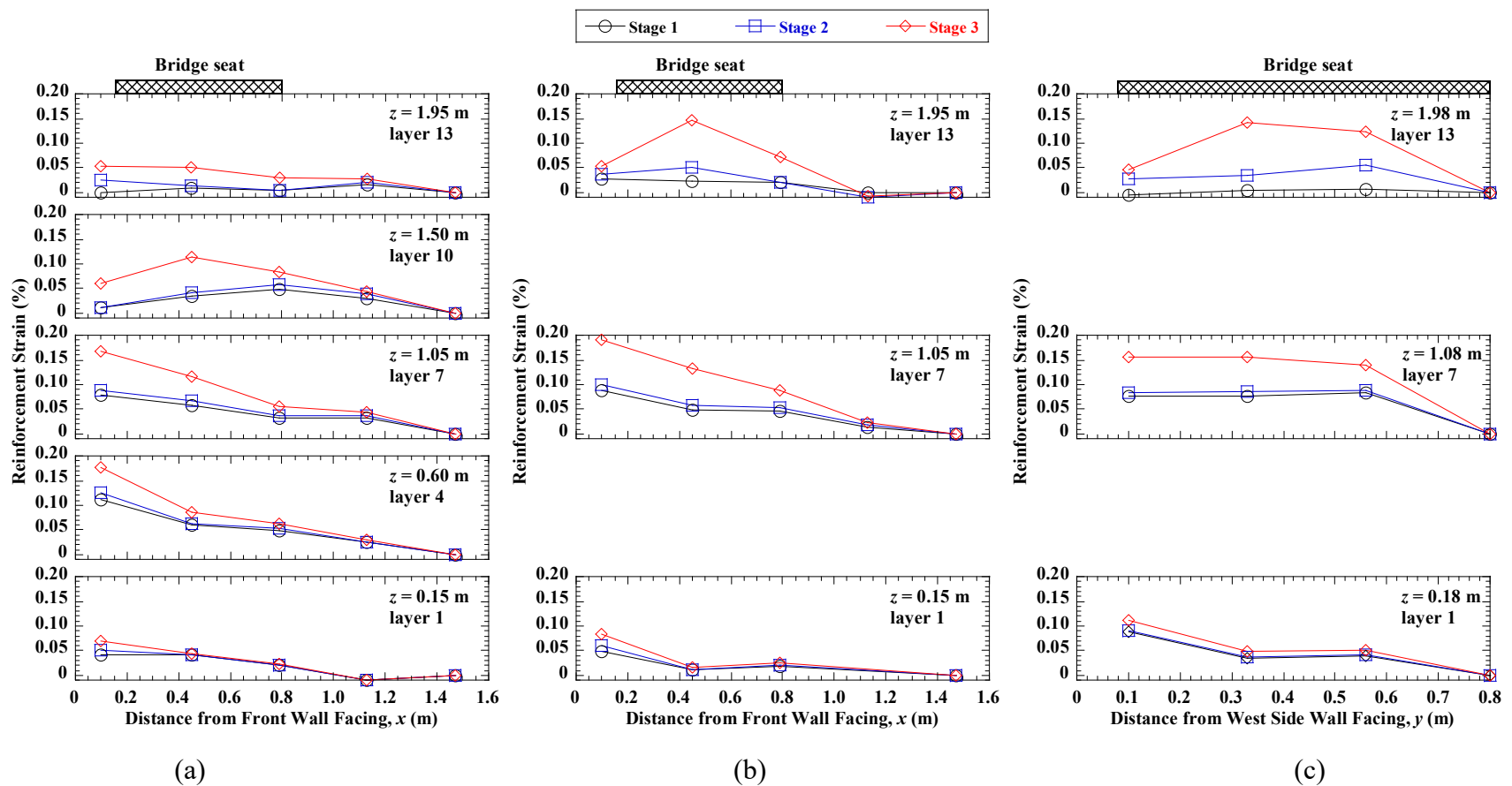


Figure 15. Distributions of tensile strain in reinforcement layers for Specimen 1: (a) L1; (b) L2; (c) T1.

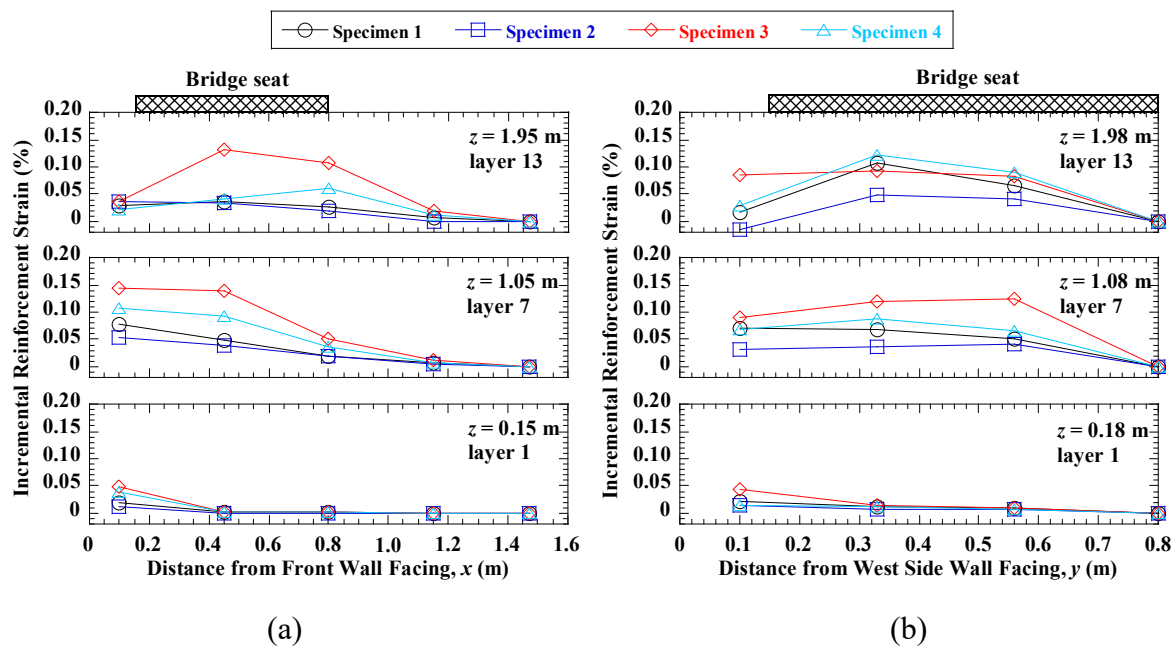


Figure 16. Distributions of incremental tensile strain in reinforcement layers due to placement of bridge beam: (a) L1; (b) T1.

List of Figure Captions

- Fig. 1.** Configuration of GRS bridge abutment system for Specimen 1.
- Fig. 2.** Specimen 1: (a) top view; (b) longitudinal cross-sectional view; (c) transverse cross-sectional view. Note: dashed lines indicate reinforcement layers perpendicular to diagram.
- Fig. 3.** Experimental results from consolidated-drained triaxial compression tests on well-graded angular sand: (a) deviator stress; (b) volumetric strain.
- Fig. 4.** Wetting-path and drying-path SWRC data with fitted relationships.
- Fig. 5.** Experimental results from tensile tests on geogrid reinforcement.
- Fig. 6.** Soil property profiles for GRS bridge abutment specimens: (a) relative density; (b) gravimetric water content.
- Fig. 7.** Instrumentation for Specimen 1: (a) longitudinal centerline section L1 ($y = 0.8$ m); (b) longitudinal off-centerline section L2 ($y = 0.35$ m); (c) transverse section T1 ($x = 0.48$ m).
- Fig. 8.** Profiles of facing displacement for front wall and longitudinal sections L1 and L2: (a) Stage 1; (b) Stage 2; (c) Stage 3.
- Fig. 9.** Profiles of facing displacement for west side wall and transverse section T1: (a) Stage 1; (b) Stage 2; (c) Stage 3.
- Fig. 10.** Maximum facing displacements: (a) L1, front wall; (b) L2, front wall; (c) T1, west side wall.
- Fig. 11.** Profiles of incremental facing displacement due to placement of bridge beam: (a) L1, front wall; (b) L2, front wall; (c) T1, west side wall.
- Fig. 12.** Time histories of settlement for bridge seat due to placement of bridge beam for Specimen 1.
- Fig. 13.** Profiles of vertical soil stress near front wall facing for longitudinal section L1: (a) Stage 1; (b) Stage 3.
- Fig. 14.** Profiles of lateral soil stress behind front wall facing for longitudinal section L1: (a) Stage 1; (b) Stage 3.
- Fig. 15.** Distributions of tensile strain in reinforcement layers for Specimen 1: (a) L1; (b) L2; (c) T1.
- Fig. 16.** Distributions of incremental tensile strain in reinforcement layers due to placement of bridge beam: (a) L1; (b) T1.

ASCE Authorship, Originality, and Copyright Transfer Agreement

Publication Title: Journal of Geotechnical and Geoenvironmental Engineering

Manuscript Title: Physical Model Tests on Half-Scale Geosynthetic Reinforced Soil Bridge Abutments. I: Static Loading

Author(s) – Names, postal addresses, and e-mail addresses of all authors

Yewei Zheng, Department of Structural Engineering, University of California, San Diego, La Jolla, CA, 92093-0085 USA. Email: y7zheng@ucsd.edu

Patrick J. Fox, Department of Civil and Environmental Engineering, Pennsylvania State University, University Park, PA, 16802 USA. Email: pjfox@engr.psu.edu

P. Benson Shing, Department of Structural Engineering, University of California, San Diego, La Jolla, CA, 92093-0085 USA. Email: pshing@ucsd.edu

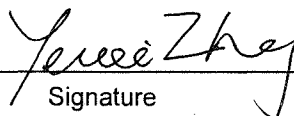
John S. McCartney, Department of Structural Engineering, University of California, San Diego, La Jolla, CA, 92093-0085 USA. Email: mccartney@ucsd.edu

I. Authorship Responsibility

To protect the integrity of authorship, only people who have significantly contributed to the research or project and manuscript preparation shall be listed as coauthors. The corresponding author attests to the fact that anyone named as a coauthor has seen the final version of the manuscript and has agreed to its submission for publication. Deceased persons who meet the criteria for coauthorship shall be included, with a footnote reporting date of death. No fictitious name shall be given as an author or coauthor. An author who submits a manuscript for publication accepts responsibility for having properly included all, and only, qualified coauthors.

I, the corresponding author, confirm that the authors listed on the manuscript are aware of their authorship status and qualify to be authors on the manuscript according to the guidelines above.

Yewei Zheng



06/04/18

Print Name

Signature

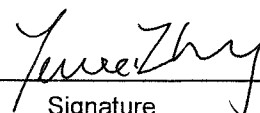
Date

II. Originality of Content

ASCE respects the copyright ownership of other publishers. ASCE requires authors to obtain permission from the copyright holder to reproduce any material that (1) they did not create themselves and/or (2) has been previously published, to include the authors' own work for which copyright was transferred to an entity other than ASCE. Each author has a responsibility to identify materials that require permission by including a citation in the figure or table caption or in extracted text. Materials re-used from an open access repository or in the public domain must still include a citation and URL, if applicable. At the time of submission, authors must provide verification that the copyright owner will permit re-use by a commercial publisher in print and electronic forms with worldwide distribution. For Conference Proceeding manuscripts submitted through the ASCE online submission system, authors are asked to verify that they have permission to re-use content where applicable. Written permissions are not required at submission but must be provided to ASCE if requested. Regardless of acceptance, no manuscript or part of a manuscript will be published by ASCE without proper verification of all necessary permissions to re-use. ASCE accepts no responsibility for verifying permissions provided by the author. Any breach of copyright will result in retraction of the published manuscript.

I, the corresponding author, confirm that all of the content, figures (drawings, charts, photographs, etc.), and tables in the submitted work are either original work created by the authors listed on the manuscript or work for which permission to re-use has been obtained from the creator. For any figures, tables, or text blocks exceeding 100 words from a journal article or 500 words from a book, written permission from the copyright holder has been obtained and supplied with the submission.

Yewei Zheng



06/04/18

Print name

Signature

Date

III. Copyright Transfer

ASCE requires that authors or their agents assign copyright to ASCE for all original content published by ASCE. The author(s) warrant(s) that the above-cited manuscript is the original work of the author(s) and has never been published in its present form.

The undersigned, with the consent of all authors, hereby transfers, to the extent that there is copyright to be transferred, the exclusive copyright interest in the above-cited manuscript (subsequently called the "work") in this and all subsequent editions of the work (to include closures and errata), and in derivatives, translations, or ancillaries, in English and in foreign translations, in all formats and media of expression now known or later developed, including electronic, to the American Society of Civil Engineers subject to the following:

- The undersigned author and all coauthors retain the right to revise, adapt, prepare derivative works, present orally, or distribute the work, provided that all such use is for the personal noncommercial benefit of the author(s) and is consistent with any prior contractual agreement between the undersigned and/or coauthors and their employer(s).
- No proprietary right other than copyright is claimed by ASCE.
- If the manuscript is not accepted for publication by ASCE or is withdrawn by the author prior to publication (online or in print), or if the author opts for open-access publishing during production (journals only), this transfer will be null and void.
- Authors may post a PDF of the ASCE-published version of their work on their employers' **Intranet** with password protection. The following statement must appear with the work: "This material may be downloaded for personal use only. Any other use requires prior permission of the American Society of Civil Engineers."
- Authors may post the **final draft** of their work on open, unrestricted Internet sites or deposit it in an institutional repository when the draft contains a link to the published version at www.ascelibrary.org. "Final draft" means the version submitted to ASCE after peer review and prior to copyediting or other ASCE production activities; it does not include the copyedited version, the page proof, a PDF, or full-text HTML of the published version.

Exceptions to the Copyright Transfer policy exist in the following circumstances. Check the appropriate box below to indicate whether you are claiming an exception:

☐ **U.S. GOVERNMENT EMPLOYEES:** Work prepared by U.S. Government employees in their official capacities is not subject to copyright in the United States. Such authors must place their work in the public domain, meaning that it can be freely copied, republished, or redistributed. In order for the work to be placed in the public domain, ALL AUTHORS must be official U.S. Government employees. If at least one author is not a U.S. Government employee, copyright must be transferred to ASCE by that author.

☐ **CROWN GOVERNMENT COPYRIGHT:** Whereby a work is prepared by officers of the Crown Government in their official capacities, the Crown Government reserves its own copyright under national law. If ALL AUTHORS on the manuscript are Crown Government employees, copyright cannot be transferred to ASCE; however, ASCE is given the following nonexclusive rights: (1) to use, print, and/or publish in any language and any format, print and electronic, the above-mentioned work or any part thereof, provided that the name of the author and the Crown Government affiliation is clearly indicated; (2) to grant the same rights to others to print or publish the work; and (3) to collect royalty fees. ALL AUTHORS must be official Crown Government employees in order to claim this exemption in its entirety. If at least one author is not a Crown Government employee, copyright must be transferred to ASCE by that author.

☐ **WORK-FOR-HIRE:** Privately employed authors who have prepared works in their official capacity as employees must also transfer copyright to ASCE; however, their employer retains the rights to revise, adapt, prepare derivative works, publish, reprint, reproduce, and distribute the work provided that such use is for the promotion of its business enterprise and does not imply the endorsement of ASCE. In this instance, an authorized agent from the authors' employer must sign the form below.

☐ **U.S. GOVERNMENT CONTRACTORS:** Work prepared by authors under a contract for the U.S. Government (e.g., U.S. Government labs) may or may not be subject to copyright transfer. Authors must refer to their contractor agreement. For works that qualify as U.S. Government works by a contractor, ASCE acknowledges that the U.S. Government retains a nonexclusive, paid-up, irrevocable, worldwide license to publish or reproduce this work for U.S. Government purposes only. This policy DOES NOT apply to work created with U.S. Government grants.

I, the corresponding author, acting with consent of all authors listed on the manuscript, hereby transfer copyright or claim exemption to transfer copyright of the work as indicated above to the American Society of Civil Engineers.

Yewei Zheng

Print Name of Author or Agent



Signature of Author or Agent

06/04/18

Date

More information regarding the policies of ASCE can be found at <http://www.asce.org/authorsandeditors>

Authors: Zheng, Fox, Shing, and McCartney

Technical Paper: JGGE GTENG 7258

Title: Physical Model Tests of Half-Scale Geosynthetic Reinforced Soil Bridge Abutments. I: Static Loading

Date: April 2019

Response to Review Comments

Editor:

I received your original manuscript titled: “Physical Model Tests on Half-Scale Geosynthetic Reinforced Soil Bridge Abutments. II: Static Loading” (GTENG-7258-R1) for possible publication in the ASCE Journal of Geotechnical and Geoenvironmental Engineering (JGGE). Your Technical Paper (TP) presents the results of static laboratory tests on half-scale geosynthetic reinforced soil (GRS) bridge abutments to investigate the measured stresses, strains, and displacements of the GRS abutment after construction and due to the placement of a model bridge and additional static loads. The applied loads are really small so the measured stresses, strains, and displacements are also really small, which makes the applicability of the results limited.

Three (3) highly active reviewers in this field have reviewed your manuscript and their extensive review comments are provided below. Based on these many and significant review comments, the Associate Editor (AE) recommended that your revised manuscript be “Accept As Is”.

As an Editor of the JGGE, I also have reviewed your TP great interest in the subject matter and do not concur with the AE's recommendation because Reviewer #4 “declined” your paper and thinks the field data on the seismic response should be moved to your companion paper or the importance of the measurements better explained in this paper. In addition, it appears that about 40% of this manuscript is covered in your companion paper GTENG-7259 and your other publications, e.g., Zheng et al. (2018d). Please delineate the new or unpublished information in this paper?

Accordingly, the decision regarding publication is deferred until a revised manuscript has been submitted and I have re-reviewed it. If the comments from all of the reviewers have been addressed satisfactorily, I will send it to Reviewer #4 for re-review. This decision provides you and your co-authors with an opportunity to address the various review comments, proofread the TP, improve some of the explanations and conclusions, combine or delete figures, and strengthen

your predicted versus measured data comparisons and conclusions. The reviewers have provided detailed comments and suggestions that will assist you in this revision process. Please carefully address all of the review comments from Reviewer #4 and provide a TABULATED point-by-point response along with your revised manuscript.

Response: We value the reviewers' comments and the opportunity to revise the manuscript, and have added more explanations to improve the manuscript.

These papers present a unique study of physical model tests on GRS bridge abutments with different configurations under working stress, static loading conditions to understand the multi-directional response of this type of 3D structures in a controlled laboratory setting in a systematic manner, which has not been investigated before. The experimental data from this study provides needed background for the shaking table tests described in the companion paper, and also information suitable for validation of 3D numerical models.

With regard to possible overlap of materials – all of the experimental results in this paper (i.e., static response of 4 different abutment specimens from Figure 8 to Figure 16) are new and have not been previously published, and also are not found in our companion paper (which presents corresponding dynamic response results) or the GTJ (Zheng et al. 2018a) and the GI (Zheng et al. 2018b) papers. Nonetheless, we have carefully gone through the text to ensure that the only remaining overlap with the GTJ paper focusing on experimental design and the GI paper focusing on transverse shaking is the necessary descriptions of materials and test specimens. This amount of overlap is necessary for the paper to be “stand alone” quality, as ASCE requires.

With regard to the magnitude of applied stresses, our experiments involve stresses that are representative of single-span bridges under service load conditions. We have added a statement in the text to clarify this point: “These surcharge stresses are at the lower end of the typical range, yet representative of service load conditions for GRS bridge abutments supporting a single-span bridge. For example, the GRS-IBS abutment for the Huber Road Bridge reported by Adams et al. (2011a) has a similar applied surcharge stress of 73 kPa.”

Associate Editor:

The revised draft has been reviewed by the same three (3) previous reviewers. Two of them have decided that the paper to be accepted for publication. Thus, the Associate Editor made the recommendation of accepting it. However, it is hoped that the authors will consider the comments of rejection by the third reviewer before submitting it for production, such as the difference in tendency of results compared to FHWA specifications.

Response: Thank you for the recommendation and suggestion. We have added more explanations and improved the manuscript.

Reviewer #3:

This manuscript gave the monitoring results in the process of the study on the seismic response of GRS bridge abutments, which had weaker meaning than that of a static loading study on GRS abutments. Authors gave only the results, didn't analyze the why. For example, why the measured vertical soil stress is lower than that of FHWA calculation? So this article is of no theoretical meaning.

Response: Thank you for your comment on the manuscript. Although we agree that no study has evaluated the seismic response of GRS bridge abutments in different configurations as we presented in our companion paper, the same can be said regarding the understanding of the different testing configurations on the static response. This paper provides valuable data not available in the literature that can be used to better understand the static loading response of GRS bridge abutments, including the different stages of construction. To address the concern of the reviewer, we have added more explanations regarding our interpretation of the measurements in the different tests. For example, the measured vertical soil stresses in the lower section for Stage 1 compared to the calculated AASHTO (2012) values are attributed to the friction developed at the back of facing blocks and partial support of backfill soil weight from reinforcement near the facing. There are other places in the revised text where additional information is included.

References

- AASHTO. (2012). *AASHTO LRFD bridge design specifications*, 6th Edition, American Association of State Highway and Transportation Officials, Washington, D.C.
- Adams, M., Nicks, J., Stabile, T., Wu, J., Schlatter, W., and Hartmann, J. (2011). “Geosynthetic reinforced soil integrated bridge system synthesis report.” *FHWA-HRT-11-027*, U.S. DOT, Washington, D.C.
- Zheng, Y., Sander, A.C., Rong, W., Fox, P.J., Shing, P.B., and McCartney, J.S. (2018a) “Shaking table test of a half-scale geosynthetic-reinforced soil bridge abutment.” *Geotechnical Testing Journal*, 10.1520/GTJ20160268.
- Zheng, Y., McCartney, J. S., Shing, P. B., and Fox, P. J. (2018b). “Transverse shaking table test of a half-scale geosynthetic reinforced soil bridge abutment.” *Geosynthetics International*, DOI: 10.1680/jgein.18.00019.